Current Research in Immunology 2 (2021) 79–92

Contents lists available at ScienceDirect

Current Research in Immunology

journal homepage: www.editorialmanager.com/crimmu/Default.aspx

Plasmodium berghei Hsp90 contains a natural immunogenic I-A^b-restricted antigen common to rodent and human *Plasmodium* species

Matthias H. Enders [a,b,c], Ganchimeg Bayarsaikhan [d], Sonia Ghilas [a,b], Yu Cheng Chua [a], Rose May [a,b], Maria N. de Menezes [a], Zhengyu Ge [a], Peck Szee Tan [e], Anton Cozijnsen [f], Vanessa Mollard [f], Katsuyuki Yui [d], Geoffrey I. McFadden [f], Mireille H. Lahoud [e], Irina Caminschi [e], Anthony W. Purcell [e], Ralf B. Schittenhelm [e,g], Lynette Beattie [a,b,*,1], William R. Heath [a,b,*,1], Daniel Fernandez-Ruiz [a,b,*,1]

[a] *Dept. of Microbiology and Immunology, The University of Melbourne at the Peter Doherty Institute for Infection and Immunity, Melbourne, VIC, 3000, Australia*
[b] *The ARC Centre of Excellence in Advanced Molecular Imaging, University of Melbourne, Parkville, VIC, 3010, Australia*
[c] *University of Bonn, Developmental Biology of the Immune System, Life & Medical Sciences Institute (LIMES), Bonn, NRW, D-53127, Germany*
[d] *Division of Immunology, Department of Molecular Microbiology and Immunology, Graduate School of Biomedical Sciences, Nagasaki University, Sakamoto, Nagasaki, 852-8523, Japan*
[e] *Infection and Immunity Program, Monash Biomedicine Discovery Institute and Dept. of Biochemistry and Molecular Biology, Monash University, Clayton, VIC, 3800, Australia*
[f] *The School of BioSciences, University of Melbourne, Parkville, VIC, 3010, Australia*
[g] *Monash Proteomics & Metabolomics Facility, Monash University, Clayton, VIC, 3800, Australia*

ARTICLE INFO

Keywords:
CD4 T cell subsets
Plasmodium epitope
Vaccination
T cell memory
Experimental cerebral malaria
Malaria immunity

ABSTRACT

Thorough understanding of the role of CD4 T cells in immunity can be greatly assisted by the study of responses to defined specificities. This requires knowledge of *Plasmodium*-derived immunogenic epitopes, of which only a few have been identified, especially for the mouse C57BL/6 background. We recently developed a TCR transgenic mouse line, termed PbT-II, that produces CD4$^+$ T cells specific for an MHC class II (I-A^b)-restricted *Plasmodium* epitope and is responsive to both sporozoites and blood-stage *P. berghei*. Here, we identify a peptide within the *P. berghei* heat shock protein 90 as the cognate epitope recognised by PbT-II cells. We show that C57BL/6 mice infected with *P. berghei* blood-stage induce an endogenous CD4 T cell response specific for this epitope, indicating cells of similar specificity to PbT-II cells are present in the naïve repertoire. Adoptive transfer of *in vitro* activated T_H1-, or particularly T_H2-polarised PbT-II cells improved control of *P. berghei* parasitemia in C57BL/6 mice and drastically reduced the onset of experimental cerebral malaria. Our results identify a versatile, potentially protective MHC-II restricted epitope useful for exploration of CD4 T cell-mediated immunity and vaccination strategies against malaria.

1. Introduction

Malaria remains a major infectious disease threatening the health and livelihoods of hundreds of millions of people globally. Vaccination against malaria would improve the prospects for disease reduction, but a highly efficacious vaccine remains elusive (Cockburn and Seder, 2018). It is therefore essential to expand our understanding of the basic immunological mechanisms conducive to anti-malarial immunity to enable generation of novel vaccines or to improve existing strategies (Fernandez-Ruiz et al., 2021). Identification of immunogenic epitopes remains a key area for further development.

CD4 T cells intervene in a broad variety of immunological processes and have been shown to play essential roles in immunity to different developmental stages of *Plasmodium* within their mammalian host. In mice vaccinated with radiation-attenuated sporozoites, CD4 T cells are necessary to enable CD8 T cell immunity (Carvalho et al., 2002), which

Abbreviations: DC, dendritic cells; cDC1, type I conventional DC; ECM, experimental cerebral malaria; Hsp, heat shock protein.

* Corresponding authors. The ARC Centre of Excellence in Advanced Molecular Imaging, University of Melbourne, Parkville, VIC, 3010, Australia.
E-mail addresses: lynette.beattie@unimelb.edu.au (L. Beattie), wrheath@unimelb.edu.au (W.R. Heath), danielfr@unimelb.edu.au (D. Fernandez-Ruiz).
[1] Co-senior author.

https://doi.org/10.1016/j.crimmu.2021.06.002
Received 20 January 2021; Received in revised form 26 June 2021; Accepted 28 June 2021

controls liver stage *Plasmodium* infection (Fernandez-Ruiz et al., 2016; Schofield et al., 1987). CD4 T cells also contribute to the control of blood-stage infections with *P. chabaudi*, *P. yoelii* and *P. berghei* (Süss et al., 1988; Langhorne et al., 1990; Butler et al., 2011; Haque et al., 2011; Hirunpetcharat et al., 1999). This population of T cells is very diverse, able to differentiate into functionally distinct subtypes early upon activation by antigen presenting cells (APC) (Choi et al., 2013). Interactions with monocytes or B cells shortly after activation during *Plasmodium* infection polarises CD4 T cells into T_H1 or T_{FH} cells respectively (Lonnberg et al., 2017). Depletion of CD4 T cells during acute *P. chabaudi* infection, but not later, prevents mice from making parasite-specific IgG and hinders subsequent parasite control (Langhorne et al., 1990), with antibody production facilitated by Tfh-B cell interactions (Perez-Mazliah et al., 2015, 2017). T_H1 cells are also reported to modulate the growth of acute *P. chabaudi* parasitemia (Wikenheiser et al., 2016). In addition to their contribution to immunity, CD4 T cells have been also involved in the development of severe malaria pathology, namely experimental cerebral malaria (ECM) (Amante et al., 2010). This form of severe malaria pathology is triggered by the accumulation of infected red blood cells (iRBC) and parasite-specific CD8 T cells in the brain of *P. berghei* infected mice (Belnoue et al., 2002; Lundie et al., 2008; Swanson et al., 2016). The latter are thought to respond to parasite antigen on brain endothelial cells, alter the blood brain barrier, increasing its permeability and causing fatal neurological damage (Howland et al., 2013; Ghazanfari et al., 2018). CD4 T cells promote inflammation and attract pathogenic CD8 T cells to the brain during blood stage *P. berghei* infection, triggering ECM (Villegas-Mendez et al., 2012).

Understanding of CD4 T cell biology in malaria has been greatly enhanced by the development of MHC-II restricted, *Plasmodium*-specific transgenic T cells (Stephens et al., 2005; Fernandez-Ruiz et al., 2017), which enabled detailed analyses of CD4 T cell responses during infection or after vaccination. Recently, we developed the PbT-II line, an MHC-II-restricted TCR transgenic line specific for *Plasmodium*, on the C57BL/6 background (Fernandez-Ruiz et al., 2017). This line was derived from a CD4 T cell isolated from the spleen of a *P. berghei* blood-stage-infected mouse, but its cognate epitope was unknown (Fernandez-Ruiz et al., 2017). PbT-II cells responded to *P. chabaudi*, *P. yoelii*, and even to *P. falciparum* blood stage parasites, indicating their specificity for a well conserved epitope. Moreover, PbT-II cells also responded to irradiated *P. berghei* sporozoites, and hence their specific target was broadly expressed. PbT-II cells were able to elicit protective immunity to *P. chabaudi* when adoptively transferred into CD40L-deficient mice, and were able to enhance priming of *Plasmodium*-specific CD8 T cells by cDC1 (Fernandez-Ruiz et al., 2017). These properties underscored the importance of identifying the cognate epitope of PbT-II cells to enable the study of endogenous CD4 T cell responses of the same specificity during infection, a more physiological scenario than use of PbT-II cells, and to enable exploration of CD4 T cell-based vaccination against *Plasmodium* in this system.

Here, we used a mass spectrometry-based approach to identify a peptide within *P. berghei* heat shock protein 90 (*Pb*Hsp90, PBANKA_0805700), $PbHsp90_{484\text{-}496}$, as the cognate epitope recognised by PbT-II cells. We incorporated this epitope in a vaccine platform and defined its potential for protection against blood-stage *P. berghei* infection. Knowledge of this epitope also enabled us to generate *in vitro* activated PbT-II cells polarised towards T_H1 or T_H2 subtypes, which revealed a highly protective capacity of these cells against ECM and blood stage *P. berghei* infection. We conclude that $PbHsp90_{484\text{-}496}$ is a valuable epitope for the study of CD4 T cells against malaria in the C57BL/6 background.

2. Results

2.1. PbT-II cells form long-lived memory

We recently described a novel MHC-II-restricted TCR transgenic mouse line, termed PbT-II, that responds to a conserved, unidentified *Plasmodium* epitope (Fernandez-Ruiz et al., 2017). While acute responses had been measured, it was unclear whether cells of this specificity formed memory populations, an issue relevant to vaccine development. To address this issue, we adoptively transferred 50,000 PbT-II cells expressing GFP (PbT-II.GFP) into B6 host mice, infected these mice intravenously (i.v.) with 10^4 *P. berghei*-infected red blood cells (iRBC) and enumerated PbT-II cells in the spleen and inguinal lymph nodes (iLN) up to day 49 after infection (Fig. 1A–C, S1). In this type of experiment, ECM kills all mice within 2 weeks of infection. Consequently, mice were treated with chloroquine from day 5 to avoid development of ECM. Blood stage *P. berghei* infection induced extensive expansion of PbT-II cells and seeding of lymphoid organs by day 7. A progressive decline in numbers of PbT-II cells occurred thereafter, with significant numbers still remaining on day 49 (Fig. 1A and B). Virtually all effector and memory PbT-II cells expressed CD44 (Fig. 1C). In the spleen, most PbT-II cells (approximately 79% on average) were $CD62L^-$ at each time point examined, hence displaying a T_{EM} phenotype (Fig. 1C). In the inguinal lymph node, as expected, the great majority of PbT-II cells (>70%) were $CD62L^+$, as this marker is required for T cell entry to these lymphoid organs. We detected no expression of CD69 in either organ (Fig. 1C), suggesting cells were not continuously exposed to stimulation by antigen, nor formed resident memory populations in these tissues. Numbers of PbT-II cells transferred into naïve recipients remained low throughout the time course (Fig. 1A and B), with some of them showing CD44 expression early after transfer (Fig. S1C). Together, these data indicated that PbT-II cells could form memory populations in response to *P. berghei* blood-stage infection.

PbT-II cells have also been shown to respond to *P. berghei* radiation attenuated sporozoites (RAS) (Fernandez-Ruiz et al., 2017), and vaccination of mice adoptively transferred with PbT-II.GFP cells revealed memory cells persisting in the spleen 50 days post-infection (Fig. 1D). To confirm that these PbT-II cells were not simply effectors responding to persisting antigen, we evaluated the persistence of the antigen recognised by PbT-II cells after RAS infection. To do this, we transferred CTV-coated, naïve PbT-II cells at different time points (day −1, 7 or 28) after RAS vaccination and measured their proliferation in the spleen and the liver (Fig. 1E). We detected some proliferation of PbT-II cells transferred on day 7 after RAS infection, indicating that their cognate antigen was still present at this time point. However, no proliferation was detected on PbT-II cells transferred on day 28. This suggested that the PbT-II cells identified on day 50 after RAS infection were memory T cells maintained independently of continuous antigenic stimulation.

2.2. Discovery of the cognate antigen of PbT-II cells

While PbT-II cells are highly useful to study CD4 T cell responses against malaria, their cognate antigen was unknown. This prevented us from studying endogenous CD4 T cell responses of the same specificity, limiting the scope of applicability of this new tool. We therefore sought to define the cognate epitope of PbT-II cells using a mass spectrometry-based approach. To do this, we cultured large numbers of DC (obtained from C57BL/6 mice treated with Flt3 ligand-producing cells (Mach et al., 2000)) with blood stage *P. berghei* parasites for 8 h (Valencia-Hernandez et al., 2020). We then eluted MHC-II ($I\text{-}A^b$)-bound peptides from these DC and used high resolution mass spectrometry to identify *P. berghei*-derived peptides in the eluate. Using this workflow, we identified a total of 1187 epitopes derived from *P. berghei* alongside 26,578 epitopes of murine origin. 75 of these *P. berghei*-derived peptides fulfilled the following criteria and were selected for further analysis: (i) they were between 13 and 20 amino acids in length, (ii) they had been assigned a Byonic search engine score of at least 185 (which reflects the quality of peptide-spectrum matches), (iii) they were absent from naïve DC control samples, (iv) they showed either 100% sequence identity in *P. yoelii*, *P. chabaudi* and *P. falciparum*, or >90% sequence identity in *P. falciparum*. These peptides were chemically synthesised. To test their capacity to activate PbT-II cells, we enriched PbT-II.GFP cells from the spleen of a

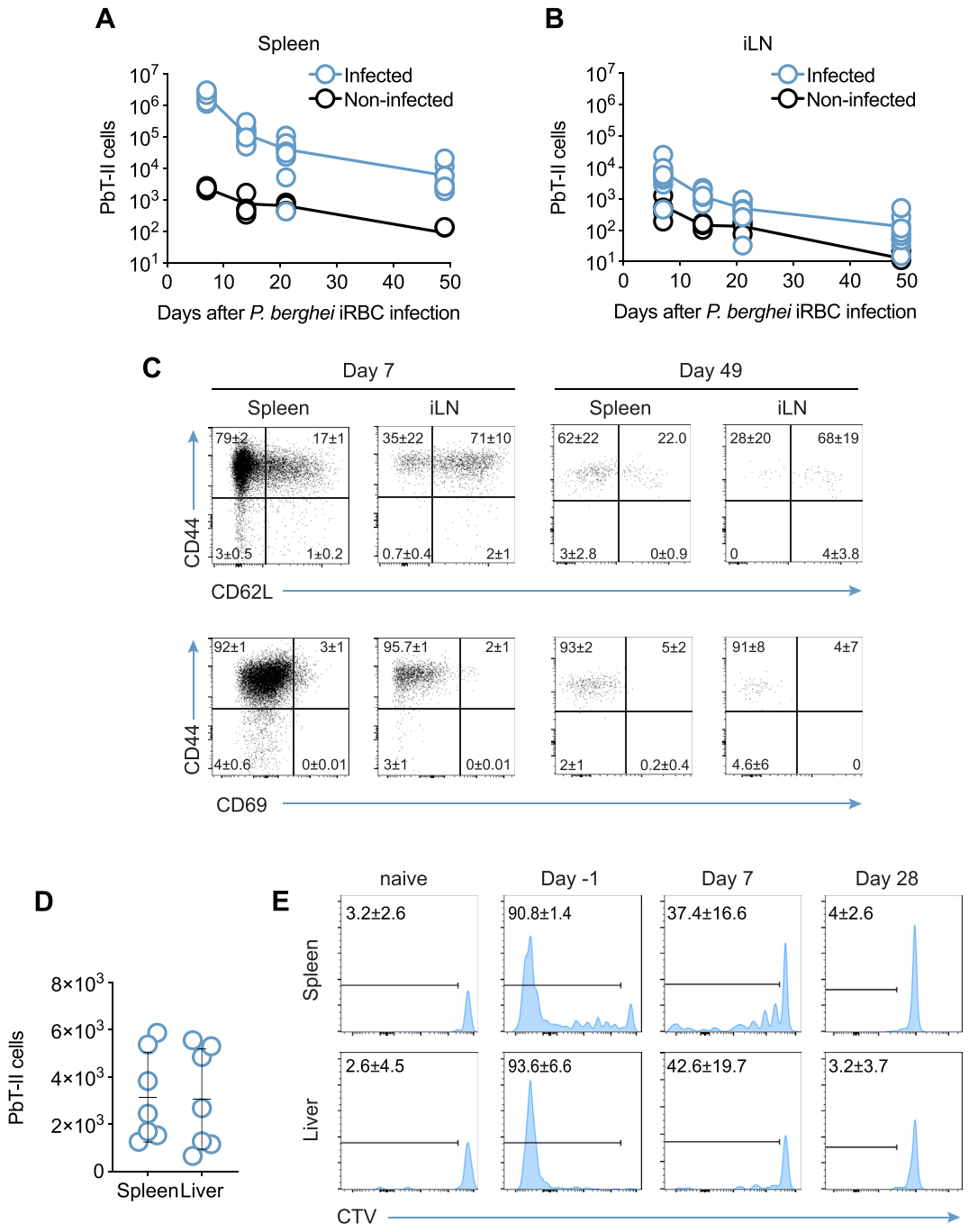

Fig. 1. ***Hsp90-specific CD4 T cells form stable memory.*** **A-B.** ***PbT-II cell expansion and memory formation after*** **P. berghei** ***iRBC infection followed by chloroquine treatment.*** Naïve, WT C57BL/6 mice received 5 × 10^4 PbT-II.GFP cells, were injected (blue) or not (black) with 10^4 *P. berghei* iRBC i.v. on the next day and were treated with chloroquine from day 5. PbT-II cells were enumerated in the spleen (**A**) and inguinal lymph nodes (**B**) on the indicated days. Data were pooled from 2 independent experiments; each one with 5 infected and 1–2 non-infected mice. ***C. Representative FACS plots of PbT-II cells*** from panels A and B, gated on days 7 or 49. Numbers represent average percentages ± SD of total CD4 T cells. ***D. Memory PbT-II cell generation after RAS immunisation***. Mice received 5 × 10^4 PbT-II.GFP cells and were infected with 5 × 10^4 *P. berghei* RAS i.v. on the next day. PbT-II cells were enumerated in the spleen and the liver 50 days after immunisation. Data were pooled from 2 independent experiments, with 2–4 mice per group and experiment. Error bars represent mean ± SD. ***E. Proliferation of PbT-II cells upon transfer into RAS immunised mice.*** Mice received 5 × 10^4 *P. berghei* RAS i.v. on day 0, and 5 × 10^5 CTV-coated PbT-II.GFP cells on days −1, 7 or 28 after RAS injection. Proliferation of PbT-II cells in the spleen and the liver was determined 5 days after injection of RAS. Representative histograms are shown. Numbers represent mean percentages of total CD4 T cells ± SD. Data are representative for 2 independent experiments, each one with 3 mice/group.

PbT-II mouse infected with *P. berghei* iRBC 8 days earlier and treated with chloroquine from day 4. We restimulated these PbT-II cells *in vitro* with a small amount of each of the chemically synthesised peptides and performed intracellular staining for IFN-γ. Peptide 58 (DNQKDIYYITGESINAVS) induced a significant upregulation of IFN-γ production in PbT-II cells (Fig. 2A and B). This peptide originates from the heat shock protein 90 (Hsp90) of *P. berghei* (PBANKA_0805700). Hsp90 is one of the most abundant chaperons and shares 94% sequence identity with its ortholog in *P. falciparum*, *Pf*Hsp90.

MHC-II molecules have an open groove from which peptides can protrude (Chicz et al., 1992), and so we next sought to define the minimal epitope capable of stimulating PbT-II cells. Smaller versions of peptide 58

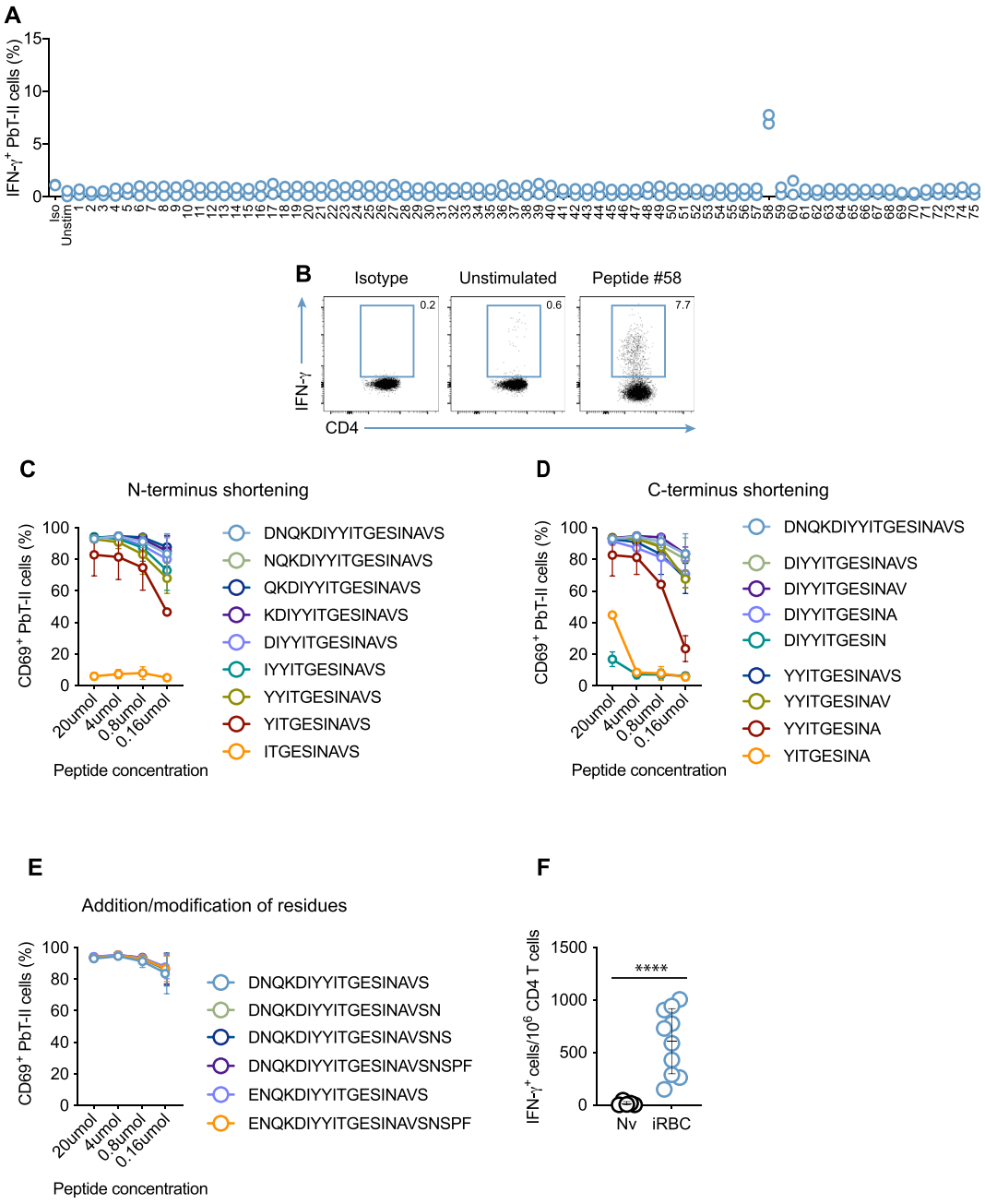

Fig. 2. ***Discovery of the cognate peptide of PbT-II cells. A,B. Identification of a* Plasmodium *peptide recognised by PbT-II cells.*** Splenocytes from a PbT-II.GFP mouse infected with 10^4 *P. berghei* iRBC i.v. 8 days earlier and treated with chloroquine from day 4 were cultured for 5 h with brefeldin A and candidate peptides at a concentration of 2.5 μM, and intracellularly stained. Cells were gated as $CD4^+$ $V\alpha2^+$ GFP^+ and IFN-γ^+. **A.** Percentages of IFN-γ^+ PbT-II cells. Data were pooled from two independent experiments. **B.** Representative FACS plots of samples in A. ***C-E. Identification of the minimal epitope recognised by PbT-II cells.*** Splenocytes from a naïve PbT-II.GFP mouse were cultured overnight with the titrated amounts of the indicated peptides and expression of CD69 was measured by flow cytometry. Data were pooled from 2 independent experiments. **C.** Subtraction of residues at the N-terminus of DNQKDIYYITGESINAVS. **D.** Subtraction of residues at the C-terminus of DNQKDIYYITGESINAVS. **E.** Responsiveness of PbT-II cells to Hsp90 epitopes larger than DNQKDIYYITGESINAVS and to their *P. falciparum* versions. Data in C-E were pooled from 2 independent experiments; error bars represent mean ± SD. ***F. Detection of Hsp90-specific endogenous CD4 T cell responses in mice exposed to blood stage* P. berghei *infection.*** Naïve WT C57BL/6 mice were infected with 10^4 *P. berghei* iRBC i.v. and were treated with chloroquine from day 5. On day 7 after infection, splenocytes were enriched for CD4 T cells and incubated with the DIY peptide for 18 h. ELISpot was performed to detect IFN-γ producing cells. Data were log transformed and compared using a Student's t-test. Two values of "0" in the control group were transformed to "1" to enable log transformation. Data are representative for two experiments, each one with 2–3 naive and 5 infected mice per group. Error bars represent mean ± SD.

shortened at their N-terminus (Fig. 2C) were synthesised and tested for their capacity to induce CD69 upregulation in naïve PbT-II cells. Peptide variant DIYYITGESINAVS provided maximal response, comparable to that elicited by peptide 58, and YYITGESINAVS was the shortest peptide version to provide a substantial response. We then tested the responsiveness of peptide variants shortened at their C-terminus. On the basis of our previous result, we used shortened versions of DIYYITGESINAVS and YYITGESINAVS. While removal of the C-terminal serine had minimal impact on the stimulatory capacity of these peptides, removal of the valine significantly diminished PbT-II responses (Fig. 2D). We conclude that the minimum epitope required for maximal stimulation of PbT-II cells is DIYYITGESINAV, or *Pb*Hsp90$_{484\text{-}496}$ (termed hereafter DIY for

simplicity), with YYITGESINAV still inducing substantial responses. We next evaluated the stimulatory capacity of Hsp90-derived peptides longer than peptide 58. Addition of at least four extra residues to the C-terminus of peptide 58 still resulted in maximal PbT-II stimulation (Fig. 2E). The sequence of peptide 58 in the *P. falciparum* ortholog of *P. berghei* Hsp90 differs from the latter in the first residue at its N-terminus, which changes from aspartic acid in *P. berghei* to glutamic acid. We found PbT-II cells to respond equally strongly to either peptide (Fig. 2E). Identification of the optimal epitope recognised by PbT-II cells allowed examination of the endogenous CD4 T cell response to this epitope. An ELISpot assay revealed splenic IFN-γ producing T cells specific for the DIY epitope were induced on day 7 after *P. berghei* blood-stage infection of B6 mice (Fig. 2F), establishing that *Pb*Hsp90-specific endogenous CD4 T cells responded to this infection.

Knowledge of the cognate peptide recognised by PbT-II cells also enabled us to target this epitope through vaccination, and to study its potential as a target for immunisation against malaria. Because cDC1 are the main antigen presenting cell for CD4 T cells in malaria

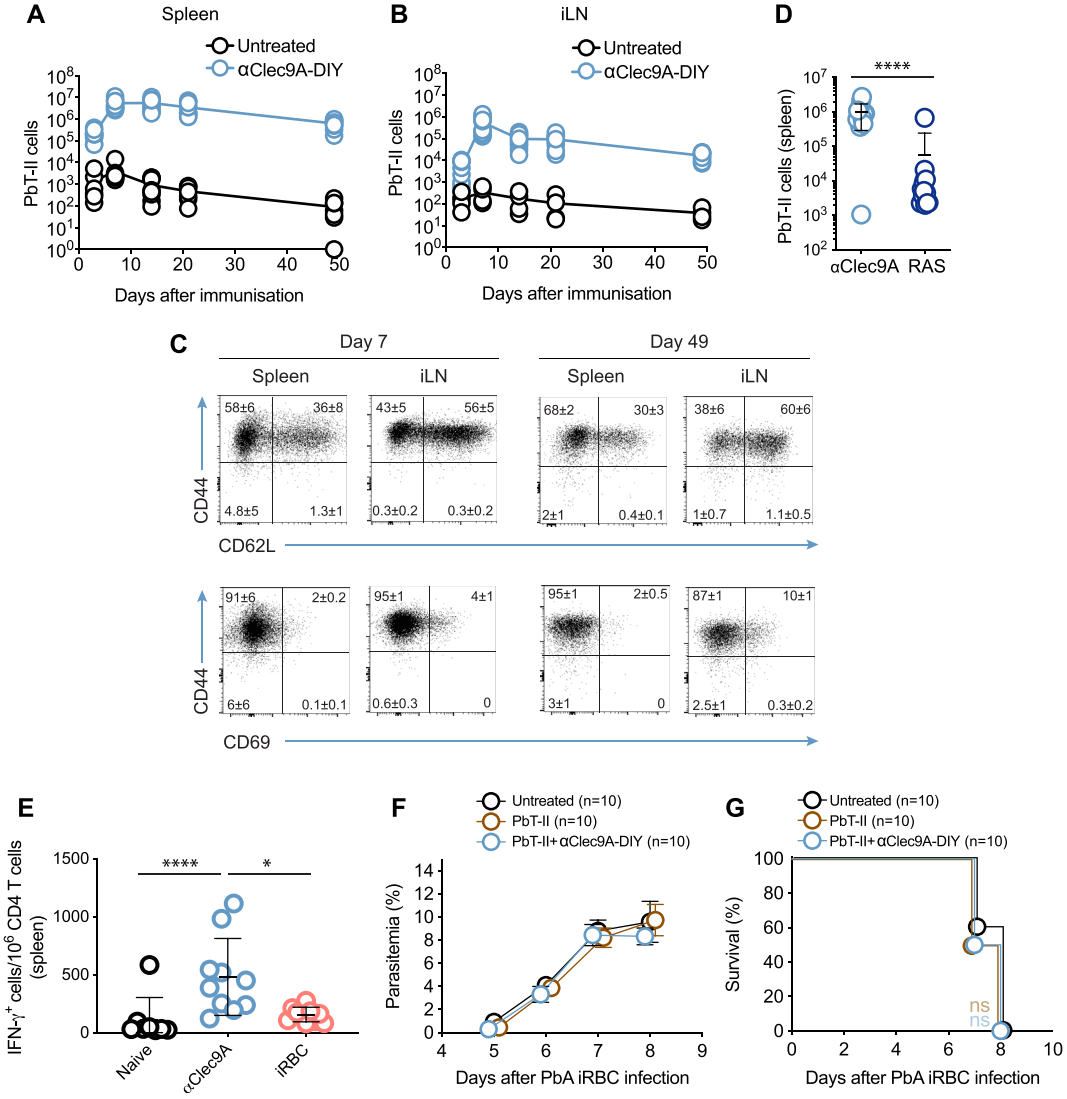

Fig. 3. ***αClec9A vaccination targeting the DIY epitope of Hsp90 induces potent memory formation. A-C. Immunisation with αClec9A-DIY induces strong PbT-II cell memory formation.*** Naïve C57BL/6 mice received 5×10^4 PbT-II.GFP cells and were immunised with 8 μg αClec9A-DIY mAb and 5 nmol CpG. Numbers of PbT-II cells were measured in the spleen (**A**) and inguinal lymph node (**B**) at the indicated time points after immunisation. Data were pooled from two independent experiments, each one with 2–4 untreated and 5 vaccinated mice per group. ***C. Representative FACS plots of PbT-II cells*** from panels A and B, gated on days 7 or 49. Numbers represent average percentages ± SD of total CD4 T cells. ***D. αClec9A vaccination induces more potent PbT-II memory than RAS.*** Mice received 5×10^4 PbT-II.GFP cells and were injected with either 2 μg αClec9A-DIY and 5 nmol CpG or 5×10^4 RAS. Numbers of memory PbT-II cells were measured in the spleen on day 28 after immunisation. Data were log-transformed and compared using a Student's t-test. Data were pooled from 2 independent experiments; with 3–10 mice/group. Error bars represent mean ± SD. ***E. Induction of a specific endogenous CD4 T cell response to the DIY epitope by αClec9A-DIY vaccination.*** Mice were immunised with 2 μg αClec9A-DIY and 5 nmol CpG or infected with 10^4 *P. berghei* iRBC and cured from day 5. On day 35 after immunisation/infection, splenocytes (including 250,000 CD4 T cells/well) were restimulated *in vitro* with the DIY peptide and ELISpot was performed to detect IFN-γ producing cells**.** Data were log-transformed and compared using one-way ANOVA and Tukey's Multiple Comparisons test. Data were pooled from 2 independent experiments; each one with 4–5 mice per group. Error bars represent mean ± SD. ***F, G. Protective capacity of αClec9A-DIY vaccination against blood stage* P. berghei *infection.*** Mice received 5×10^4 PbT-II.GFP cells and were immunised with 2 μg αClec9A-DIY and 5 nmol CpG one day later. They then were infected with 10^4 *P. berghei* iRBC 7–14 days after priming. ***F. Course of* P. berghei *parasitaemia***. Data were log-transformed and analysed using One-Way ANOVA and Dunnett's Multiple Comparisons tests comparing each group's parasitemia with that of the untreated group. No significant differences were found. ***G. Survival***. Statistical analysis of survival was carried out by performing pairwise comparisons between the different groups using log-rank tests and adjusting for multiple comparisons by performing a Bonferroni correction for the total number of groups (significance level was $P < 0.016$; n.s., $P > 0.016$). Data in F, G were pooled from 2 independent experiments, each one with 5 mice/group.

(Fernandez-Ruiz et al., 2017), we generated a reagent to shuttle the PbT-II epitope to this DC subtype for maximal responses: we conjugated the DIY epitope to a monoclonal antibody (mAb) that targets Clec9A, a canonical surface receptor of cDC1. Optimal CD4 T cell priming does not necessarily require an adjuvant (Lahoud et al., 2011), and thus we first compared the capacity of this reagent to induce the expansion of PbT-II cells, with or without CpG adjuvant, which was previously shown to be optimal for the expansion of CD8 T cells through αClec9A mAb (Fernandez-Ruiz et al., 2016). Indeed, maximal PbT-II proliferation was achieved even at lower doses of αClec9A-DIY when this mAb was administered together with CpG adjuvant (Fig. S2). We therefore decided to utilise the αClec9A-DIY reagent in combination with CpG adjuvant for subsequent experiments.

We next sought to determine the kinetics of PbT-II cell expansion and persistence after αClec9A-DIY immunisation. Mice received 50,000 PbT-II.uGFP cells and were immunised with 8 μg αClec9A-DIY and 5 nmol CpG, and PbT-II cells were enumerated and phenotyped in the spleen and inguinal lymph node up to day 49 after immunisation (Fig. 3A–C, S3). This revealed a large expansion of PbT-II cells and the formation of memory T cells in vaccinated mice (Fig. 3A and B). These cells showed a phenotype similar to that of PbT-II cells generated after iRBC infection (Figs. 3C and 1C). However, compared to blood-stage infection, the proportion of T_{CM} cells was somewhat higher in the spleen and lower in the LN (Figs. 3C and 1C), and a small but consistent population of LN PbT-II cells (~10%) expressed CD69 (Fig. 3C). The total number of memory PbT-II cells in the spleen on day 27 after immunisation using 2 μg αClec9A-DIY and 5 nmol CpG was significantly higher than that obtained in mice vaccinated with 50,000 RAS (Fig. 3D). In the absence of PbT-II cell adoptive transfer, vaccination with αClec9A-DIY also expanded an endogenous population of specific CD4 T cells and generated a significant number of memory cells (Fig. 3E). Again, αClec9A-DIY vaccinated mice generated significantly higher numbers of Hsp90-specific memory CD4 T cells than iRBC infected mice (Fig. 3E).

We showed previously that PbT-II cells can compensate for the lack of functional endogenous CD4 T cells in CD40L KO mice and, partially, in RAG KO mice, provide immunity against *P. chabaudi* infection (Fernandez-Ruiz et al., 2017). The development of the αClec9A-DIY reagent enabled us to test whether immunisation expanding these cells could improve immunity against blood stage *Plasmodium* infection. To assess this question, PbT-II/uGFP cells were adoptively transferred into B6 mice prior to vaccination with αClec9A-DIY and CpG adjuvant, and then these mice were challenged 7–14 days later with 10,000 *P. berghei* iRBC. This vaccination regime did not provide protection, however, based neither on reduced parasitaemia levels (Fig. 3F) nor the onset of ECM (Fig. 3G).

2.3. Generation of different helper phenotypes of PbT-II cells

CD4 T cells are highly heterogeneous, with modes of immunisation and adjuvants potentially inducing different types of helper phenotypes in activated effector cells. We reasoned that the failure of αClec9A-DIY vaccination in inducing protection from blood stage *P. berghei* infection might be due to the generation of effector CD4 T cell phenotypes of suboptimal efficacy against this type of infection, particularly as this approach primarily induces cells of a T_{FH} phenotype (Kato et al., 2015). The identification of the cognate epitope of PbT-II cells provided the opportunity to *in vitro* activate these cells under specific polarising conditions to generate populations of helper cells of particular phenotypes. Thus, *in vitro* activation of PbT-II cells under T_H1-polarising conditions induced approximately 90% of the activated cells to produce either IFN-γ or TNF, with 70% producing both cytokines, 7 days after transfer into recipient mice (Fig. 4A–C). In contrast, PbT-II activation under T_H2-polarising conditions induced >70% of cells to produce IL-4 or IL-13, with nearly 50% of these cells producing both cytokines. A substantial proportion of T_H2-polarised cells (above 40%) also expressed TNF. Both T_H1 and T_H2-polarised cells contained similar frequencies (approximately 55%) of IL-2 producing cells. Importantly, Th1- and Th2-polarised cells maintained their phenotype in naïve recipient mice for at least 35 days after transfer (Fig. S4).

In comparison with *in vitro*-polarised cells, PbT-II cells expanded *in vivo* by αClec9A-DIY immunisation displayed a T_H1-like phenotype on day 7, with high expression of IFN-γ, but a low percentage of these cells expressed TNF compared to T_H1-polarised cells activated *in vitro*. The phenotype of the PbT-II cells expanded after αClec9A-DIY immunisation was indeed similar to that induced by blood stage *P. berghei* infection, with the latter inducing higher percentages of IFN-γ- and TNF-producing PbT-II cells, but a similar percentage of IL-2-producing PbT-II cells. Only iRBC infection induced moderate IL-10 expression in PbT-II cells, and none of the strategies used to activate PbT-II cells induced IL-17 expression (Fig. 4A–C). In agreement with previous reports (Fernandez-Ruiz et al., 2017), a significant proportion of PbT-II cells activated during blood stage *P. berghei* infection adopted a T_{FH} phenotype (Fig. 4D–F). Indeed, this was also the case for cells activated using αClec9A-DIY, with close to 70% of the PbT-II cells expressing increased levels of CXCR5 and PD1 (Fig. 4D–F). This proportion was however not significantly higher than that induced by *P. berghei* iRBC infection (Fig. 4F). PbT-II cells activated *in vitro* under T_H1 or T_H2-polarising conditions did not develop into a Tfh phenotype (Fig. 4D–F).

We next sought to determine whether *in vitro* activated T_H1 or T_H2 PbT-II cells would differ from those generated by αClec9A-DIY immunisation in their capacity to protect mice from blood stage *P. berghei* infection. Mice received 10^7 *in vitro* activated T_H1 or T_H2 PbT-II or gDT-II cells and were challenged with 10^4 *P. berghei* iRBC 7 days after transfer. Mice that received either type of PbT-II cells developed lower levels of parasitaemia (Fig. 5A) and were significantly protected from ECM (Fig. 5B). Similar results were obtained when mice were challenged 35 days after T cell transfer (Fig. 5C and D). In this case, however, T_H2 PbT-II cells provided better protection against ECM than T_H1 cells. *In vitro* activated CD4 T cells of an irrelevant specificity (gDT-II cells) did not alter the course of parasitaemia nor influenced ECM development (Fig. 5A-D).

3. Discussion

Here, we identified *Pb*Hsp90$_{484\text{-}496}$ as the cognate antigen of PbT-II cells, opening new ways to utilise a versatile tool for the study of CD4 T cells in malaria, and enabling the study of endogenous CD4 T cells of the same specificity. Identification of this epitope enabled us to target CD4 T cells for vaccination against blood stage *Plasmodium* infection, and to generate populations of polarised PbT-II cells and test their protective capacity, revealing a protective role for T_H2 cells, and moderately for T_H1 cells, against blood stage infection.

The immunogenic epitope within *P. berghei* Hsp90 initially identified here using mass spectrometry as capable of activating PbT-II cells (peptide 58) is an 18-mer peptide (DNQKDIYYITGESINAVS) eluted from MHC-II molecules (I-A^b) of parasite-exposed DC. MHC-II molecules have an open peptide-binding groove that enables loading of large peptides, which can protrude from both sides of the cleft (Hunt et al., 1992; Brown et al., 1993). Binding of the peptide to the MHC-II molecule occurs through via a core of 9 residues containing critical anchor points. But this core 9-mer is not necessarily fixed. For instance, in some cases the same peptide can bind to MHC-II molecules in different registers, thus using different 9-mer cores (McFarland et al., 1999). However, flanking residues of the 9-mer core can influence MHC-II stability and the peptide conformation in the cleft, as well as make contact with the TCR, playing a role in its affinity for MHC-II (McFarland et al., 1999; Landais et al., 2009; Nelson et al., 1994; Holland et al., 2013). It was therefore important to identify the minimal epitope within the *Pb*Hsp90-derived 18-mer peptide initially identified by mass spec (DNQKDIYYITGESINAVS), and to determine whether additional flanking residues influenced PbT-II cell responsiveness. We conclude that the 9-mer core that mediates binding to MHC-II is YITGESINA, as deletion of any further residues on either side drastically reduced PbT-II cell stimulation. However, the 14-mer

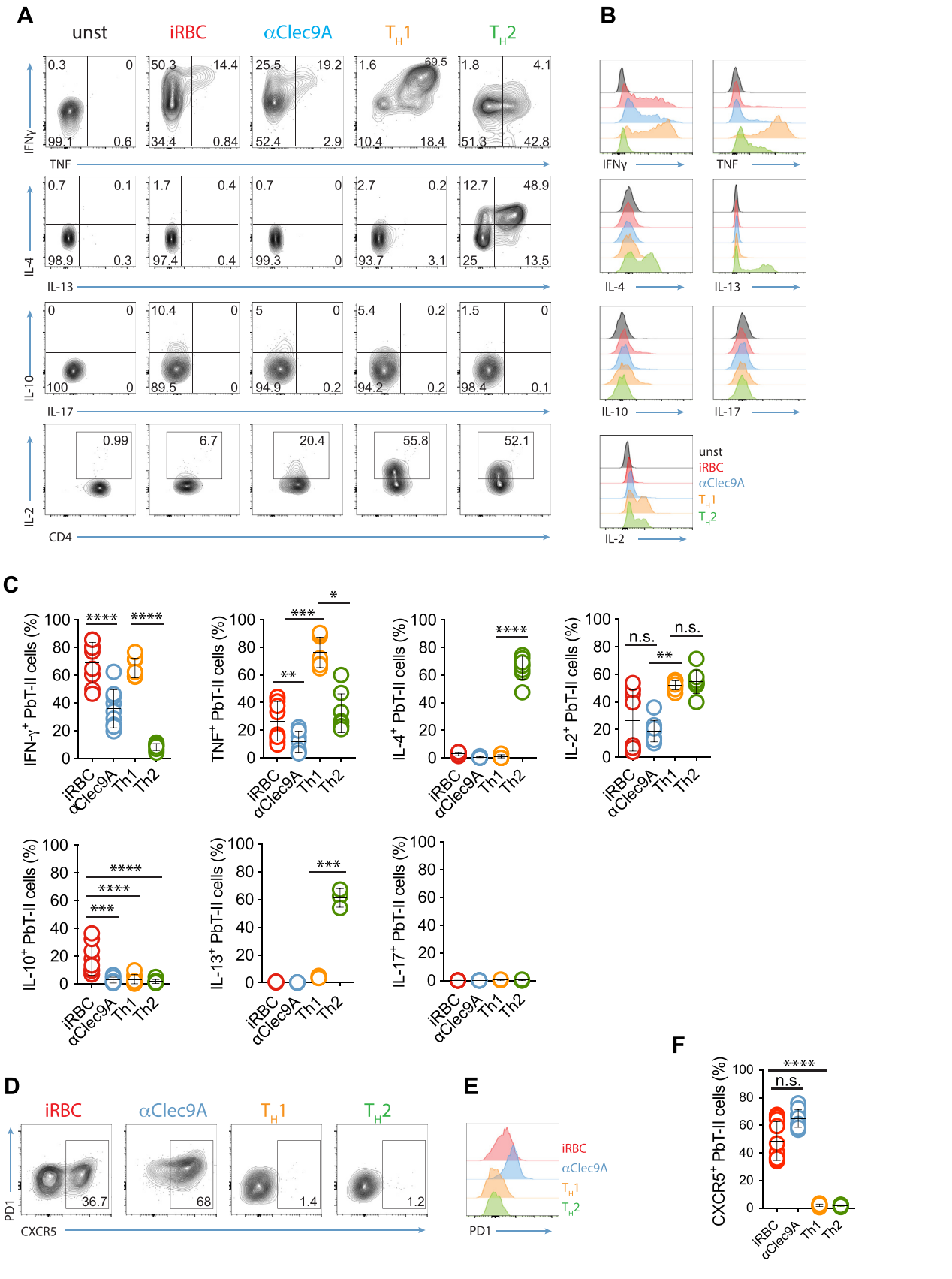

(caption on next page)

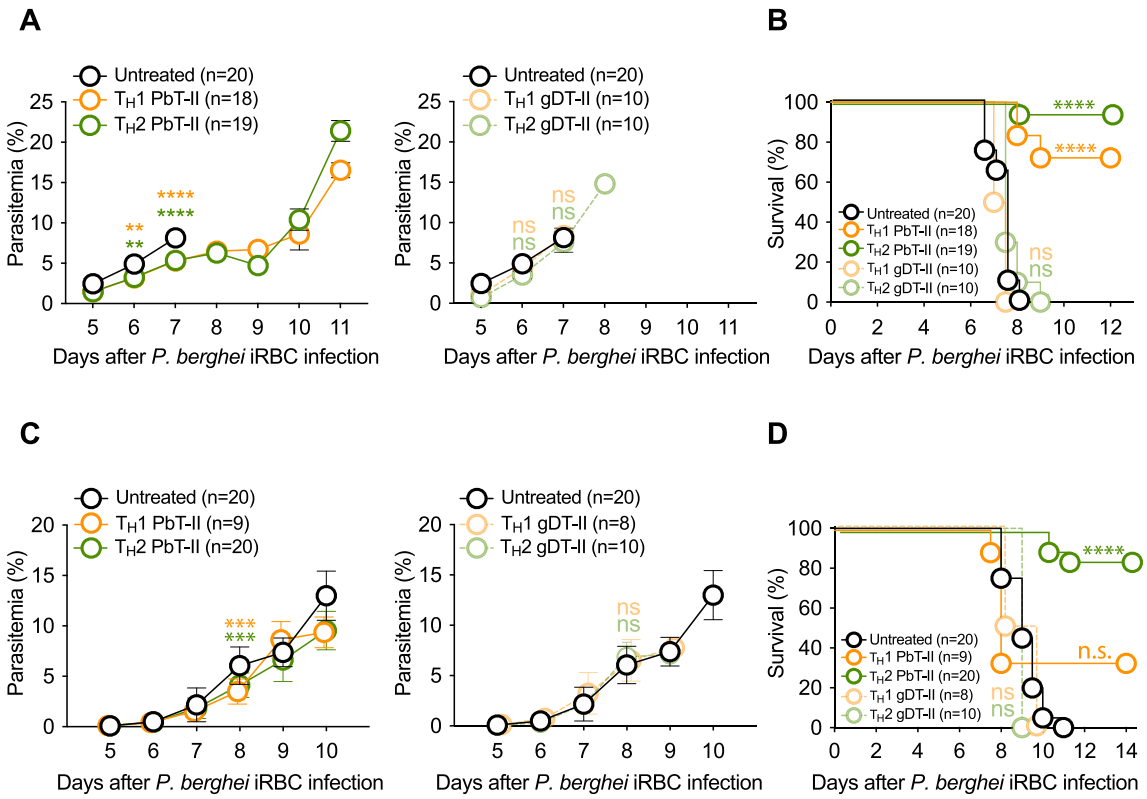

Fig. 5. ***Hsp90-specific T_H2 cells induce partial immunity to blood stage* Plasmodium spp. *infection, and ECM protection. A-D. Protective capacity of in vitro polarised T_H1 or T_H2 effector Hsp90-specific CD4 T cells on the course of* P. berghei *iRBC infection.*** Naïve C57BL/6 mice received 10^7 *in vitro* activated, T_H1- or T_H2-polarised PbT-II or control gDT-II cells and were infected with 10^4 *P. berghei* iRBC 7 days later (**A**, **B**) or 100 *P. berghei* iRBC 35 days later (**C**, **D**). **A, C.** ***Course of* P. berghei *parasitaemia*.** For clarity, test and control groups are shown in separate graphs (PbT-II, left panels; gDT-II, right panels). Data were log-transformed and analysed using One-Way ANOVA and Dunnett's Multiple Comparisons tests comparing each group's parasitemia with that of the untreated group (n.s. = not significant, $P > 0.05$; **, $P < 0.01$;, ***, $P < 0.001$; ****, $P < 0.0001$). **B, D.** ***Survival.*** Survival was analysed by performing pairwise comparisons between the different groups using log-rank tests and adjusting for multiple comparisons by performing a Bonferroni correction for the total number of groups (significance level was $P < 0.01$; n.s., $P > 0.01$; ****, $P < 0.0001$). Data were pooled from 2 to 3 independent experiments for the untreated, Th1- and Th2-PbT-II groups, and 1–2 experiments for Th1- and Th2-gDT-II groups, with 4–10 mice/group.

DIYYITGESINAVS, including extra residues at both the N- and the C-termini of the 9-mer core peptide, provided the highest stimulation of PbT-II cells. Remarkably, addition of further residues to this 14-mer, either to the N- or the C-termini, up to a total of at least 22 residues, still resulted in maximal PbT-II cell responsiveness, suggesting that these residues likely protrude outside the region of interaction between the MHC-II molecule and the TCR and neither are necessary, nor obstruct, PbT-II recognition of Hsp90. Also, post administration digestion of these larger peptides may contribute to their stimulatory capacity. In any case, this feature has broader implications in vaccination seeking to generate *Plasmodium*-specific CD4 T cell responses. As shown here for *P. falciparum* Hsp90, residue variation outside the 9-mer core between orthologs across different parasites does not appear to affect immunogenicity, enabling the target of multiple *Plasmodium* species through subunit vaccination containing relatively small epitopes, as long as the MHC-binding core epitope is maintained. Moreover, larger peptides may contain multiple core registers presentable by different HLA molecules, thus broadening immunogenicity in human populations.

Hsp90 is an essential, highly conserved and abundant protein in all eukaryotic organisms, including *Plasmodium* parasites, which consists of different subtypes. *Pb*Hsp90 (PBANKA_0805700) has a relatively high sequence identity (66%) with both mouse Hsp90α (*Hsp90aa1*) and Hsp90β (*Hsp90ab1*). The peptide DIYYITGESINAVS in *Pb*Hsp90 changes to **HIYFITGE**TKDQVA in mouse Hsp90α (50% identity) and to **SIYYIT-GES**KEQVA in mouse Hsp90β (64% identity). Similarly, *P. falciparum* Hsp90 (Pf3D7_0708400) has 68% and 64% sequence identity with human Hsp90α and Hsp90β respectively (PlasmoDB). Hsp90 is conserved across several parasitic protists such as *Plasmodium*, *Toxoplasma*, *Trypanosoma* or *Leishmania* and this is reflected in the fact that growth of parasites as diverse as *P. falciparum*, *P. berghei*, *Toxoplasma gondii*, and *Trypanosoma evansi* can be inhibited by geldanamycin, a structural analog of ATP that interferes with Hsp90 function (Pallavi et al., 2010;

Fig. 4. ***Phenotype of PbT-II cells activated* in vitro *or generated after* P. berghei *iRBC infection or αClec9A immunisation. A-C. Characterisation of activated PbT-II cells.*** Naïve C57BL/6 mice received 5×10^4 PbT-II.GFP cells and were infected with 10^4 *P. berghei* iRBC, or immunised with 2 μg αClec9A-DIY and 5 nmol CpG one day later (αClec9A), or received 2×10^6 PbT-II cells activated *in vitro* under T_H1- or T_H2-polarising conditions. IFN-γ, TNF, IL-4, IL-13, IL-10, IL-17 and IL-2 levels in PbT-II cells from the spleen were examined by intracellular staining on day 7 after infection/immunisation/adoptive cell transfer. Unst = unstained intracellularly. **A.** Representative dot plots. **B.** Representative histograms. **C.** Percentages of PbT-II cells expressing the indicated cytokines. **D-F.** ***Determination of the proportion of Tfh cells.*** Additional samples were stained for CXCR5 and PD1 to estimate proportions of Tfh cells generated. **D.** Representative contour plots. **E.** Representative histograms for PD1 expression. **F.** Proportions of Tfh cells generated. Fig. 4A and B are representative for the data shown in Fig. 4C. Fig. 4D and E are representative for the data shown in Fig. 4F. Data in Fig. 4C and F were pooled from 2 independent experiments for IL-2, IL-4, IFN-γ and IL-10. IL-17 and IL-13 expression was examined in one experiment. Each experiment included 3–5 mice per group. Error bars in 4C and 4F denote mean ± SD. Data were log-transformed and analysed using one-way ANOVA and tukey's Multiple Comparisons tests. n.s. = not significant, $P > 0.05$; *, $P < 0.05$; **, $P < 0.01$;, ***, $P < 0.001$; ****, $P < 0.0001$.

Echeverria et al., 2005; Banumathy et al., 2003). *Pf*Hsp90 associates with other proteins, such as Hsp70, via an adaptor protein (Banumathy et al., 2003; Gitau et al., 2012) to function as an ATP-dependent chaperon, contributing to the folding of newly synthesised proteins and cell growth, and to mediating signal transduction (Pratt, 1997; Daniyan et al., 2019). Interestingly, Hsp90 stabilises ribosomal subunit components (Kim et al., 2006), another abundant group of *Plasmodium* proteins that coincidentally contain protective CD8 T cell epitopes (Valencia-Hernandez et al., 2020). *Pf*Hsp90 is predominantly present in the cytoplasm of the parasite (Gitau et al., 2012), and, unlike other heat shock proteins, it has not been found within the exportome to the host's RBC (Sargeant et al., 2006). Nevertheless, this does not diminish its immunogenic properties, as APC can take up parasites and present internal proteins to CD4 T cells via MHC-II molecules (Fernandez-Ruiz et al., 2017; Arroyo and Pepper, 2020). Indeed, while the intracellular location of Hsp90 impedes its targeting by antibodies, *Pb*Hsp90-specific PbT-II cells can still activate B cells of other specificities for isotype switching and the production of high affinity, protective antibodies (Fernandez-Ruiz et al., 2017). Importantly, the immunogenicity of *Pb*Hsp90$_{484\text{-}496}$ upon natural iRBC infection seems moderate (approximately 0.05% of total endogenous splenic CD4 T cells in *P. berghei* infected mice specific for this epitope, Fig. 2F) compared to that previously established for dominant MHC-II *P. berghei* epitopes such as ENTRAMP, GADPH or EF1α (roughly 0.1–0.5% of total CD4 T cells in *P. berghei* infected mice) (Draheim et al., 2017). This could reflect differences in the expression of these antigens (Draheim et al., 2017), or may reflect a relative scarcity of *Pb*Hsp90$_{484\text{-}496}$-specific precursors in the naïve CD4 T cell repertoire of B6 mice compared to these other specificities. However, this did not hinder our capacity to efficiently expand *Pb*Hsp90$_{484\text{-}496}$-specific cells and generate robust memory through αClec9A vaccination, supporting the suitability of this antigen as a target for vaccination studies.

CD4 T cells are important mediators of immunity against blood stage *Plasmodium* infection (Perez-Mazliah and Langhorne, 2014). Subpopulations of parasite-specific T_H1 and Tfh CD4 T cells form shortly after blood stage *P. berghei* and *P. chabaudi* infection (Lonnberg et al., 2017; Fernandez-Ruiz et al., 2017). T_H1 cells appear to contribute to the modulation of the peak of *P. chabaudi* parasitemia during acute infection (Wikenheiser et al., 2016; James et al., 2018) and also reduce *P. berghei* parasitemia (Oakley et al., 2013), although impaired capacity to generate T_H1 cells translates into better control of non-lethal *P. yoelii* parasitemia (Oakley et al., 2014; Salles et al., 2017). While modulation of *P. berghei* parasitemia by CD4 T cells in C57BL/6 mice does not impede lethality early after infection, *P. chabaudi* parasitaemia progresses to a persistent stage in WT mice once a prominent first peak is reduced to almost undetectable levels. Tfh cells, acting during the acute stage of infection, are essential for the generation of efficient humoral responses capable of eliminating persistent infection (Perez-Mazliah et al., 2015, 2017). Similarly, Tfh cells are also critical for control of persistent parasitemia by non-lethal *P. yoelii* infections (Zander et al., 2015). Here, we tested the protective capacity of vaccination targeting Clec9A against *P. berghei*, using recombinant mAb linked to the *Pb*Hsp90 epitope, combined with a CpG-based adjuvant. This form of vaccination is known to elicit strong T_{FH} and humoral responses (Lahoud et al., 2011), and we indeed achieved strong formation of Tfh cells, as well as moderate generation of T_H1 cells capable of co-expressing IFN-γ and TNF (Fig. 4A, D). This vaccination strategy did not exert any detectable protection of B6 mice infected with *P. berghei*. αClec9A vaccination perhaps generated insufficient numbers of T_H1 cells for substantial protection, and Tfh formation through vaccination may not have provided a substantial advantage of over natural, endogenous Tfh formation during the course of infection.

Identification of the *Pb*Hsp90 epitope enabled us to generate highly enriched populations of T_H1-polarised PbT-II cells *in vitro* and explore their protective capacity upon adoptive transfer in a scenario in which these cells were present at high numbers, in the absence of other T_H cell populations. Production of IFN-γ (Su and Stevenson, 2000; van der Heyde et al., 1997) and TNF (Amante et al., 2010; Li and Langhorne, 2000) contributes to the control of acute *P. berghei* and *P. chabaudi* parasitemia and, in agreement with these studies, we found that adoptive transfer of high numbers of T_H1 cells expressing these cytokines significantly improved parasitemia control in the *P. berghei* blood stage infection model. Vaccination strategies that promote strong T_H1 bias, as shown for example though induction of OX-40 signalling in effector CD4 T cells (Zander et al., 2015), may hence be more effective in controlling parasitemia than αClec9A+CpG. However, as mentioned, a T_{FH} component is likely still necessary, as excessive T_H1 bias and prevention of T_{FH} formation can abrogate parasitemia control (Zander et al., 2015).

Unexpectedly, T_H1-polarised PbT-II cells reduced development of ECM. IFN-γ-producing CD4 T cells have been implicated in promoting ECM in *P. berghei*-infected B6 mice by attracting effector CD8 T cells to the brain (Villegas-Mendez et al., 2012). Lack of expression of the T_H1 transcription factor Tbet results in lower accumulation of CD4 and CD8 T cells in the brain and no ECM (Oakley et al., 2013). While ECM can occur in B6 mice in the absence of CD4 T cells (Nitcheu et al., 2003), and hence these cells are not essential, it is possible that additional numbers of Th1 cells in the spleen retained CD8 T cells in this organ through the production of IFN-γ and prevented their migration to the brain (Teo et al., 2018). Improved control of parasitemia by T_H1 PbT-II T cells may have reduced parasite accumulation in the brain, hindering ECM development, as previously reported for mice in which absence of type I IFN signalling resulted in enhanced T_H1 generation (Haque et al., 2011).

Improved control of *P. berghei* parasitemia, as well as reduction of ECM rates, was also found after adoptive transfer of T_H2-polarised PbT-II cells. T_H2 cells have been long known to form during *P. chabaudi* infection (Langhorne et al., 1989). Interactions with B cells promote T_H2 polarization in this model, and an absence of B cells results in the exclusive generation of T_H1 cells (Taylor-Robinson and Phillips, 1994; Langhorne et al., 1998). T_H2 cells were found to mediate *P. chabaudi* parasitemia control (Taylor-Robinson et al., 1993), and IL-4 KO mice, while able to control parasitemia, suffered a higher peak of acute parasitemia and a more prolonged chronic infection than their WT counterparts (von der Weid et al., 1994). Our data aligns with these studies, supporting a protective role for T_H2 cells in control of *P. berghei* blood stage infection. As for T_H1 cells, enhanced control of parasitemia by T_H2 cells, may have resulted in ECM impairment by reducing parasite loads in the brain. *P. berghei* infection does not seem to naturally induce substantial T_H2 cell polarization ((Fernandez-Ruiz et al., 2017); Fig. 4A–C), and hence adoptive transfer of *in vitro* polarised cells, or vaccination studies, remain the best strategies to study these cells in the context of *P. berghei* infection. While, as for blood stage infection, αClec9A vaccination combined with CpG adjuvant did not promote T_H2 formation, use of T_H2-promoting adjuvants or antigen targeting to cDC2, which favour the generation of these cells (Kasahara and Clark, 2012; Sponaas et al., 2006), may enable exploiting the protective capacity of T_H2 cells against *Plasmodium* spp. parasitemia. Alternatively, antigen specificity can bias *Plasmodium*-specific CD4 T cell development towards T_H1 or T_H2 (Quin and Langhorne, 2001) and, while *Pb*Hsp90$_{484\text{-}496}$ does not appear to naturally favour the formation of T_H2 cells, other T cell specificities or antigen formulations may be easily harnessed through vaccination for T_H2-mediated protection.

An aspect, not explored here, that presents a potential advantage of targeting *Plasmodium* Hsp90 for CD4 T cell immunity derives from the fact that this protein is expressed during both the liver and the blood stage of the infection (Fernandez-Ruiz et al., 2017; Howick et al., 2019). In addition to their aforementioned effects on blood stage immunity, CD4 T cells can directly kill liver stage parasites (Tsuji et al., 1990), and are required for the generation of protective memory CD8 T cell responses in the liver after RAS vaccination (Carvalho et al., 2002; Weiss et al., 1993). Therefore, vaccination aimed at stimulating CD4 T cells in combination of CD8 T cells may strengthen immunity against *Plasmodium* in the liver, while additionally protecting against blood stage infection, thus providing broader protection.

In summary, we identified here an immunogenic I-A^b-restricted

epitope in *Pb*Hsp90 that is highly conserved across *Plasmodium* species. This epitope joins a growing list of known *Plasmodium* epitopes (Draheim et al., 2017) to improve understanding of the role of CD4 T cells in malaria immunity.

4. Materials and methods

4.1. Mice

All procedures were performed in strict accordance with the recommendations of the Australian code of practice for the care and use of animals for scientific purposes. The protocols were approved by the Melbourne Health Research Animal Ethics Committee, University of Melbourne (ethic project IDs: 1112347, 1513505, 1714302, 1814522).

Female C57BL/6 (B6), GFP (Okabe et al., 1997), PbT-II (Fernandez-Ruiz et al., 2017), gDT-II (Bedoui et al., 2009), were used between 6 and 12 weeks of age. Unless otherwise specified in the figure legends, naïve WT C57BL/6 mice were used as recipients of cells, immunisation or infection in the experiments described. Mice were maintained at the specific pathogen free (SPF) Bioresources Facility (BRF) at the Department of Microbiology and Immunology (DMI), The University of Melbourne. Mice were bred onsite or purchased from the Animal Resources Center (Canning Vale, Australia). The health status of mouse lines was routinely checked by the DMI's BRF staff. Mice were housed with littermates of the same sex (up to 5 mice per box) in Tecniplast Green Line™ independently ventilated cages (IVC system; Tecniplast, Buguggiate, Italy) and kept on a regular 12-h light/dark cycle at a temperature ranging from 19 to 22 °C. Barastoc Irradiated food pellets (Ridley, Melbourne, Australia) and reverse osmosis (RO) purified water were available *ad libitum*, with water provided by a central system integrated into the rack or by sipper sacks™ (Avidity Science, Waterford, USA). Corn cob or alpha-dry were used as bedding material and environmental enrichment for nesting and play was provided. Cages were cleaned fortnightly. Experiments were carried out under pathogen-free conditions and mice were randomly assigned to experimental groups. Experimental mice were routinely monitored for appearance and behavior throughout experiments. Animals used for the generation of the sporozoites were 4-5-week-old male Swiss Webster mice purchased from the Monash Animal Services (Melbourne, Victoria, Australia) and maintained at the School of Botany, The University of Melbourne, Australia.

4.2. Mosquitoes

Anopheles stephensi mosquitoes (strain STE2/MRA-128 from BEI Resources, The Malaria Research and Reference Reagent Resource Center) were reared as described (Benedict, 1997): They were maintained at 27 °C and 75%–80% humidity with a 12 h light and dark photo-period in filtered drinking water (Frantelle beverages, Australia). The larvae were bred in plastic food trays (P.O.S.M Pty Ltd, Australia) containing 300 larvae, each with regular water changes every 3 days, and fed with Sera Vipan Baby fish food (Sera, Heinsberg, Germany). Upon eclosion, the adult mosquitoes were transferred to aluminium cages (BioQuip Products, Inc., Rancho Dominguez, CA, USA) and kept in a secure incubator (Conviron, Winnipeg, Canada), in the insectary at the same temperature and humidity and maintained on 10% sucrose.

4.3. Parasites and infections

Plasmodium berghei ANKA (BEI Resources, MRA-871) were used for infections. Sporozoites were generated for RAS vaccination as follows: Infections of naive Swiss mice were carried out by i.p inoculation of *P. berghei*-infected RBCs obtained from a donor mouse between the first and fourth passages from a cryopreserved stock. Parasitemia was monitored by Giemsa smear and exflagellation quantified 3 days post infection. 1 μL of tail prick blood was mixed with 100 μL of exflagellation media (RPMI, [ThermoFisher] supplemented with 10%v/v fetal calf serum [FCS], pH 8.4), incubated for 15 min at 20 °C, and exflagellation events per 10^4 red blood cells were counted. *A. stephensi* mosquitoes were allowed to feed on anaesthetised mice once the exflagellation rate reached 12–15 events per 10^4 red blood cells. 22 days after blood meal, salivary glands were dissected and checked for the presence of sporozoites. Sporozoites were resuspended in cold PBS and irradiated using 20,000 Rad, and were injected intravenously (i.v.) as indicated in the figure legend.

For blood stage infections, donor mice were injected with frozen stabilates of blood stage parasites. 3–7 days later, these mice were bled, their parasitemia was measured and recipient mice were injected i.v. with the indicated amount of *P. berghei* infected red blood cells (iRBC) diluted in 0.2 mL PBS. Parasitemia was assessed by microscopic analysis of blood smears or by flow cytometry (see below).

For curing, mice were injected intraperitoneally with 0.8 mg chloroquine for 5 consecutive days, starting on the day after infection indicated in the figure legend, followed by provision of drinking water containing 600 mg/L chloroquine for 3 extra days.

4.4. Generation and monitoring of ECM

Mice infected with blood-stage *P. berghei* and left untreated were monitored daily for the development of ECM. Mice were considered to have ECM when showing signs of neurological symptoms such as ataxia and paralysis, evaluated as the inability of mice to self-right.

4.5. Adoptive transfer of $CD4^+$ T cells

PbT-II and gDT-II $CD4^+$ T cells were negatively enriched from the spleens and lymph nodes of PbT-II/uGFP or gDT-II mice as described (Smith et al., 2003). Briefly, tissues were disrupted by passage through 70 μm cell strainers and red cells were lysed. Single cell suspensions were labelled with a cocktail of rat monoclonal antibodies (WEHI Antibody Services, Melbourne, Australia) specific for CD8 (clone 53-6.7), MHC Class II (clone M5/114), macrophages and dendritic cells (clones BM8 [anti-F4/80] and M1/70 [anti-CD11b]) granulocytes (clone RB6-8C5 [anti-Gr1]) and red blood cells (clone Ter119 [anti-Ter-119]) prior to incubation with BioMag goat anti-rat IgG magnetic beads (Qiagen, Hilden, Germany) and separation of labelled, non-CD4 T cells using a magnet. Enriched naïve PbT-II $CD4^+$ T cells were counted and their purity was analysed by staining with anti-CD4, anti-Vα2 and anti-Vβ12 TCR antibodies. Negatively enriched gDT-II/uGFP cells were then positively enriched using the Invitrogen Dynabeads/DETACHaBEAD Mouse CD4 Kit (Life Technologie AS, Oslo, Norway) following the manufacturer's instructions. Cell counts were adjusted to 2.5×10^5/mL in PBS and 0.2 mL were injected i.v. into recipient mice. In some instances, cells were labelled with CellTrace Violet (Thermo Fisher) prior to transfer following the manufacturer's instructions.

4.6. Dendritic cell isolation

Dendritic cells were purified from the spleens of mice as previously described (Vremec et al., 2000): spleens were finely minced and digested in 1 mg/ml collagenase 3 (Worthington Biochemical Corporation, Lakewood, NJ, USA) and 20 μg/ml DNAse I (Roche Diagnostics Deutchland, Mannheim, Germany) under intermittent agitation for 20 min at room temperature (RT). DC-T cell complexes were then disrupted by adding EDTA (pH 7.2) to the digest to a final concentration of 7.9 mM and continuing the incubation for an additional 5 min. After removing undigested fragments by filtering through a 70 μm mesh, cells were resuspended in 5 ml of 1.077 g/cm^3 isosmotic nycodenz medium (Nycomed Pharma AS, Oslo, Norway), layered over 5 ml nycodenz medium, overlayed with 1–2 ml of FCS, then centrifuged at 1700×*g* at 4 °C for 12 min. DC were resuspended in complete RPMI medium supplemented with 10% FCS before use in functional assays.

4.7. αClec9A vaccination

B6 mice were injected i.v. with the indicated doses of rat αClec9A mAb (clone 24/04-10B4) genetically fused to KDNQK**DIYYITGESINAV**SNSPFLEA, containing the *Pb*Hsp90$_{484-496}$ epitope, highlighted in bold) via a 4 Alanine linker to make the αClec9A-DIY mAb construct. αClec9A was injected with 5 nmol of a CpG oligonucleotide (CpG) generated by linking (5′ to 3') CpG-2006 to CpG-21798 (Krieg, 2006; Samulowitz et al., 2010) (Integrated DNA Technologies, Coralville, IA, USA).

4.8. In vitro activation and polarization of PbT-II cells

10^6 PbT-II or gDT-II splenocytes were cultured *in vitro* for 4–5 days together with 10^7 naive B6 DC enriched as above. These DC had been coated for 30 min at 37 °C with 2 μM *Pb*Hsp90$_{484-496}$ (DIYYITGESINAV) or gDT-II$_{315-327}$ (IPPNWHIPSIQDA) peptide (Genscript) in complete media (RPMI containing 10% FCS, 2 mM L-glutamine, 5 mM HEPES and 50 mM 2-mercaptoethanol (Sigma Aldrich, Castle Hill, NSW, Australia), in the presence of 1 μg/ml LPS (Sigma). Polarization was done as follows: T_H1 polarization was induced by adding 1 μg/ml LPS (Sigma), 10 U/ml IL-2 (Peprotech, Mt Waverly, VIC, Australia), 5 μg/ml αIL-4 mAb (11B11; Bio X Cell), and 5 ng/ml IL-12 (Biolegend) to the culture media. T_H2 polarization was induced by adding 10 U/ml recombinant human IL-2 (Peprotech, Mt Waverly, VIC, Australia), 60 ng/ml IL-4 (Biolegend), and 5 μg/ml αIFN-γ (XMG1.2, Bio X Cell) to the culture media. On day 3 of culture 15 ml of fresh complete media, including the polarization reagents as described, were added to the cultures.

Prior to transfer, cells were washed extensively with PBS to remove any excess LPS, counted and their purity analysed by staining with antibodies against CD4 and Vα2, Vβ12, Vα3.2, Tbet and Gata3. Activated cells were adjusted to the required concentration and injected in a volume of 0.2 mL of PBS via the tail vein.

4.9. Organ processing for T cell analysis

Tissues were pushed through 70 μm strainers to generate single cell suspensions. For spleen cell preparations, red blood cells were lysed and remaining cells were filtered through a 70 μm mesh. Liver cell suspensions were passed through a 70 μm mesh and resuspended in 35% isotonic Percoll. Cells were then centrifuged at 500 g for 20 min at room temperature (RT), the pellet harvested and then red cells lysed before further analysis.

4.10. Flow cytometry

CD4 (RM4-5), PD1 (J43) CXCR5 (2G8), IFN-γ (4S.B3), IL-10 (JES5-16E3), IL-17 (TC11-18H10.1), IL-2 (JES6-1A12), Vβ12 (MR11-1), Tbet (4B10) purchased from BioLegend (BioLegend, San Diego, CA, USA), CD8α (53-6.7), TCRβ (H57-597) CD44 (IM7), Vα2 (B20.1), IL-4 (11B11), TNF (MP6-XT22), GATA3 (L50-823) were purchased from Becton Dickinson (BD, Franklin Lakes, NJ, USA); CD62L (MEL-14), CD69 (H1.2F3), Vα3.2 (RR3-16), IL-13 (eBio13A) from ThermoFisher Scientific (Waltham, MA, USA).

Peptides were purchased from GenScript (Piscataway, NJ, USA). Dead cells were excluded by propidium iodide, Ghost Dye™Red 780 (Tonbo Biosciences) or LIVE/DEAD™ Fixable Near-IR Dead cell Stain Kit (Thermo Fisher Scientific) staining following the manufacturer's instructions. For the analysis of memory $CD4^+$ T cell populations in the spleen and the iLN, PbT-II $CD4^+$ $CD44^{hi}$ cells were subdivided into T_{CM} or T_{EM} based on CD62L expression (T_{CM} $CD62L^+$, T_{EM} $CD62L^-$).

Parasitaemia was assessed by incubating ~2 μl tail blood with a 5 pg/mL Hoechst 33258 solution (ThermoFisher Scientific) in FACS buffer for 1 h at 37 °C. Parasites were discriminated from uninfected RBC using a 405 violet laser and a 450/50 filter. Cells were analysed by flow cytometry on a FACS Canto or Fortessa (BD Immunocytometry Systems, San Jose, CA, USA), using FACSDiva (BD Immunocytometry Systems) or Flowjo software (Tree Star, Ashland, OR, USA).

Intracellular transcription factor staining was performed using the BD Pharmingen™ Transcription Factor Buffer set, following the manufacturer's instructions. Intracellular cytokine staining was performed using the BD Cytofix/Cytoperm™ Fixation/Permeabilization Kit, following the manufacturer's instructions, on *in vitro* restimulated cells. 1-2x10^6 cells/well were restimulated *in vitro* for 5 h at 37 °C in the presence of 2 μM *Pb*Hsp90$_{484-496}$ peptide. Brefeldin A (10 μg/mL) was added 1 h after the start of the culture. Intracellular staining was performed at 4 °C overnight.

4.11. Assessment of PbT-II activation in vitro

PbT-II cells enriched from the spleens and lymph nodes of PbT-II mice as explained before were adjusted to 10^7 cells/mL in PBS containing 0.1% BSA (Sigma). CellTrace™ violet (CTV, Thermofisher) was then used to coat PbT-II cells: 40 μL DMSO/vial were used to reconstitute lyophilised CTV stock. Then, 0.5 μL CTV per mL of cells were added, and cells were incubated for 10 min at 37 °C, followed by two washes in RPMI containing 2.5% FCS.

DC (6.5×10^5) were incubated with the indicated amounts of peptide, or with 6 μL of each of the fractions generated by liquid chromatography, for 1 h prior to adding 50,000 CTV-coated PbT-II.GFP cells per well. Upregulation of CD69 overnight were measured in PbT-II cells using flow cytometry.

4.12. Generation of Plasmodium-derived epitopes for LC-MS/MS analysis

Generation of *Plasmodium*-derived peptides was done as described before (Valencia-Hernandez et al., 2020). B6 mice were treated with FMS-like tyrosine kinase 3 receptor ligand (Flt3-L) to promote cDC1 formation. Flt3-L was given by subcutaneous injection of 10^6 Flt3-L-expressing B6 myeloma cells (Mach et al., 2000) 11 days prior to harvesting spleens and enriching for DC as explained above. Blood stage malaria parasites were used as an abundant source of antigen that is known to be recognised by PbT-II cells (Fernandez-Ruiz et al., 2017): donor B6 mice were infected with *P. berghei* iRBC and heart bled when parasitaemia levels were >15%. 2.22×10^9 splenic cells from Flt3-L-treated mice (containing 63% DC, defined as $CD11c^{hi}$ $MHC\text{-}II^{hi}$ cells) were cultured with 19.88×10^9 blood stage *P. berghei* parasites in complete RPMI media containing 10% FCS for 8 h at 37 °C and 6.5% CO2 in T175 flasks (ThermoFisher). The uninfected sample was generated in the same way, by culturing 1.66×10^9 splenic cells from Flt3-L-treated mice (containing 65.1% $CD11c^{hi}$ $MHC\text{-}II^{hi}$ cells) with 57×10^9 RBC from naïve B6 mice. Cells were then snap frozen prior to further analysis.

4.13. Analysis of MHC bound epitopes by LC-MS/MS

MHC class II bound peptides were isolated from DC by immunoaffinity chromatography and RP-HPLC essentially as described before (Schittenhelm et al., 2015). In brief, the cells were lysed in 0.5% IGEPAL, 50 mM Tris-HCl pH 8.0, 150 mM NaCl and protease inhibitors (Complete Protease Inhibitor Cocktail Tablet; Roche Applied Science, Penzberg, Germany) for 45 min at 4 °C and lysates were cleared by ultracentrifugation at 40.000 g. MHC I-A^b molecules were immunoaffinity purified using the Y-3P mouse monoclonal antibody bound to protein A sepharose. The peptides were eluted under mild acetic conditions and separated on a 50 mm monolithic C18 reverse-phase high-performance liquid chromatography (HPLC) column (Chromolith SpeedROD; Merck, Kenilworth, NJ, USA) using an EttanLC HPLC system (GE Healthcare). 90 individual fractions were collected and equidistantly pooled into 10 samples, which were vacuum concentrated and reconstituted to 15 μl with 0.1% formic acid (FA).

Using a Dionex UltiMate 3000 RSLCnano system equipped with a Dionex UltiMate 3000 RS autosampler, the fractions were loaded via an

Acclaim PepMap 100 trap column (100 μm × 2 cm, nanoViper, C18, 5 μm, 100 Å; Thermo Scientific) onto an Acclaim PepMap RSLC analytical column (75 μm × 50 cm, nanoViper, C18, 2 μm, 100 Å; Thermo Scientific). The peptides were separated by increasing concentrations of 80% ACN/0.1% FA at a flow of 250 nl/min for 95 min and analysed with a QExactive Plus mass spectrometer (Thermo Scientific). In each cycle, a full ms1 scan (resolution: 70.000; AGC target: 3e6; maximum IT: 50 ms; scan range: 375–1600 m/z) preceded up to 12 subsequent ms2 scans (resolution: 17.500; AGC target: 2e5; maximum IT: 150 ms; isolation window: 1.8 m/z; scan range: 200–2000 m/z; NCE: 27). To minimize repeated sequencing of the same peptides, the dynamic exclusion was set to 15 s and the 'exclude isotopes' option was activated.

Acquired mass spectrometric.raw files were searched against a combined UniProtKB/SwissProt database containing both mouse and *P. berghei* protein sequences. The search engine Byonic (Protein Metrics) was used to obtain peptide sequence information. Only peptides, which fell below at a false discovery rate (FDR) of 5% based on a decoy database were considered for further analysis.

4.14. Detection of PbHsp90-restricted responses by ELISpot

B6 mice were injected with 10^4 *P. berghei* iRBC and cured by chloroquine treatment from day 5, or with 2 μg αClec9A-DIY plus 5 nmol CpG, 7 or 35 days before splenocytes were collected for ELISpot analysis. 0.45 μm MultiScreen-IP sterile, clear Filter Plates (Merck) were coated overnight with 3 μg/mL IFN-γ capture Ab (clone AN-18; WEHI Antibody Services) in PBS and blocked with RPMI containing 10% FCS for 30 min at RT. Then, 2×10^5 enriched CD4 T cells (day 7; cells were enriched as explained above; see PbT-II cell enrichment) or unenriched splenocytes containing 2.5×10^5 CD4 T cells (day35) from the spleens of immunised mice were plated and cultured 18 h at 37 °C and 5% CO_2 in a humidified incubator in the presence or absence (day7) of DIY peptide (*Pb*Hsp90$_{484\text{-}496}$) or HSV-1 peptide (gD$_{315\text{–}327}$) (day35).

Plates were then incubated for 2 h with 1 μg/mL biotin-conjugated detection mAb (clone R4-6A2; WEHI Antibody Services) diluted in PBS containing 0.5% FCS, followed by incubation with Streptavidin-HRP (MabTech, Stockholm, Sweden) for 1 h at RT and with TMB substrate (MabTech) for 15 min. Plates were washed after each incubation step. An AID ELISpot reader (Advanced Imaging Devices GmbH, Strassberg, Germany) was used to enumerate spots.

4.15. Statistical analyses

Figures were generated using GraphPad Prism 8 (GraphPad Software, San Diego, CA, USA). Data are shown as mean values ± standard deviation (SD), unless otherwise stated. Statistical analyses were performed using GraphPad Prism 8. Unless otherwise indicated, data shown in the figures were pooled from all independent experiments performed. Unless otherwise stated, statistical comparisons of cell numbers in different groups were performed by log-transforming the data and using a Student's t-test (2 groups) or one-way ANOVA followed by Tukey's multiple comparisons test (>2 groups). $P < 0.05$ was considered to indicate statistical significance. *,$P < 0.05$; **,$P < 0.01$; ***, $P < 0.001$; ****, $P < 0.0001$; n.s., not significant ($P > 0.05$).

Credit author statement

Investigation: MHE, GB, SG, YCC, RM, RBS, LB, DFR; Conceptualization: DFR, WRH, LB, RBS, AWP, MHL, IC; Funding Acquisition: DFR, WRH, AWP; Resources: PST, AC, VM, GIM, MHL, IC; Supervision: MHL, IC, KY, AWP, LB, WRH, DFR; Writing original draft: DFR; Writing – review and editing: MHE, YCC, GIM, AWP, MHL, IC, LB, WRH, DFR

Declaration of competing interest

The authors declare that they have no known competing financial interests or personal relationships that could have appeared to influence the work reported in this paper.

6. Acknowledgements

We thank the members of the Mueller, Mackay and Heath labs for discussion, Melanie Damtsis and Ming Li for technical assistance, and the Doherty's animal facility staff for mice husbandryWe acknowledge the Monash Proteomics & Metabolomics Facility (MPMF) for the provision of technical support and infrastructure, which has been enabled by Bioplatforms Australia (BPA) and the National Collaborative Research Infrastructure Strategy (NCRIS).

Appendix A. Supplementary data

Supplementary data to this article can be found online at https://doi.org/10.1016/j.crimmu.2021.06.002.

7. Funding sources

This work was supported by the National Health and Medical Research Council of Australia; DFR (NHMRC 1139486), WRH (NHMRC 1154457, NHMRC 1113293, NHMRC 1124706), IC (NHMRC 1124706), AWP (NHMRC PRF 1137739) and the Australian Research Council; WRH (ARC CE140100011).

References

Amante, F.H., Haque, A., Stanley, A.C., Rivera Fde, L., Randall, L.M., Wilson, Y.A., Yeo, G., Pieper, C., Crabb, B.S., de Koning-Ward, T.F., et al., 2010. Immune-mediated mechanisms of parasite tissue sequestration during experimental cerebral malaria. J. Immunol. 185, 3632–3642.

Arroyo, E.N., Pepper, M., 2020. B cells are sufficient to prime the dominant CD4+ Tfh response to Plasmodium infection. J. Exp. Med. 217.

Banumathy, G., Singh, V., Pavithra, S.R., Tatu, U., 2003. Heat shock protein 90 function is essential for Plasmodium falciparum growth in human erythrocytes. J. Biol. Chem. 278, 18336–18345.

Bedoui, S., Whitney, P.G., Waithman, J., Eidsmo, L., Wakim, L., Caminschi, I., Allan, R.S., Wojtasiak, M., Shortman, K., Carbone, F.R., et al., 2009. Cross-presentation of viral and self antigens by skin-derived CD103+ dendritic cells. Nat. Immunol. 10, 488–495.

Belnoue, E., Kayibanda, M., Vigário, A.M., Deschemin, J.-C., Van Rooijen, N., Viguier, M., Snounou, G., Renia, L., 2002. On the pathogenic role of brain-sequestered alphabeta CD8+ T cells in experimental cerebral malaria. J. Immunol. 169, 6369–6375. Baltimore, Md. : 1950.

Benedict, M.Q., 1997. Care and maintenance of anopheline mosquito colonies. In: Crampton, J.M., Beard, C.B., Louis, C. (Eds.), The Molecular Biology of Insect Disease Vectors. Springer, Dordrecht, pp. 3–12.

Brown, J.H., Jardetzky, T.S., Gorga, J.C., Stern, L.J., Urban, R.G., Strominger, J.L., Wiley, D.C., 1993. Three-dimensional structure of the human class II histocompatibility antigen HLA-DR1. Nature 364, 33–39.

Butler, N.S., Moebius, J., Pewe, L.L., Traore, B., Doumbo, O.K., Tygrett, L.T., Waldschmidt, T.J., Crompton, P.D., Harty, J.T., 2011. Therapeutic blockade of PD-L1 and LAG-3 rapidly clears established blood-stage Plasmodium infection. Nat. Immunol. 13, 188–195.

Carvalho, L.H., Sano, G., Hafalla, J.C., Morrot, A., Curotto de Lafaille, M.A., Zavala, F., 2002. IL-4-secreting CD4+ T cells are crucial to the development of CD8+ T-cell responses against malaria liver stages. Nat. Med. 8, 166–170.

Chicz, R.M., Urban, R.G., Lane, W.S., Gorga, J.C., Stern, L.J., Vignali, D.A., Strominger, J.L., 1992. Predominant naturally processed peptides bound to HLA-DR1 are derived from MHC-related molecules and are heterogeneous in size. Nature 358, 764–768.

Choi, Y.S., Yang, J.A., Yusuf, I., Johnston, R.J., Greenbaum, J., Peters, B., Crotty, S., 2013. Bcl6 expressing follicular helper CD4 T cells are fate committed early and have the capacity to form memory. J. Immunol. 190, 4014–4026.

Cockburn, I.A., Seder, R.A., 2018. Malaria prevention: from immunological concepts to effective vaccines and protective antibodies. Nat. Immunol. 19, 1199–1211.

Daniyan, M.O., Przyborski, J.M., Shonhai, A., 2019. Partners in mischief: functional networks of heat shock proteins of Plasmodium falciparum and their influence on parasite virulence. Biomolecules 9.

Draheim, M., Wlodarczyk, M.F., Crozat, K., Saliou, J.M., Alayi, T.D., Tomavo, S., Hassan, A., Salvioni, A., Demarta-Gatsi, C., Sidney, J., et al., 2017. Profiling MHC II immunopeptidome of blood-stage malaria reveals that cDC1 control the functionality of parasite-specific CD4 T cells. EMBO Mol. Med. 9, 1605–1621.

Echeverria, P.C., Matrajt, M., Harb, O.S., Zappia, M.P., Costas, M.A., Roos, D.S., Dubremetz, J.F., Angel, S.O., 2005. Toxoplasma gondii Hsp90 is a potential drug

target whose expression and subcellular localization are developmentally regulated. J. Mol. Biol. 350, 723–734.
Fernandez-Ruiz, D., Ng, W.Y., Holz, L.E., Ma, J.Z., Zaid, A., Wong, Y.C., Lau, L.S., Mollard, V., Cozijnsen, A., Collins, N., et al., 2016. Liver-resident memory CD8(+) T cells form a front-line defense against malaria liver-stage infection. Immunity 45, 889–902.
Fernandez-Ruiz, D., Lau, L.S., Ghazanfari, N., Jones, C.M., Ng, W.Y., Davey, G.M., Berthold, D., Holz, L., Kato, Y., Enders, M.H., et al., 2017. Development of a novel CD4(+) TCR transgenic line that reveals a dominant role for CD8(+) dendritic cells and CD40 signaling in the generation of helper and CTL responses to blood-stage malaria. J. Immunol. 199, 4165–4179.
Fernandez-Ruiz, D., de Menezes, M.N., Holz, L.E., Ghilas, S., Heath, W.R., Beattie, L., 2021. Harnessing liver-resident memory T cells for protection against malaria. Expert Rev. Vaccines 20, 127–141.
Ghazanfari, N., Mueller, S.N., Heath, W.R., 2018. Cerebral malaria in mouse and man. Front. Immunol. 9, 2016.
Gitau, G.W., Mandal, P., Blatch, G.L., Przyborski, J., Shonhai, A., 2012. Characterisation of the Plasmodium falciparum hsp70-hsp90 organising protein (PfHop). Cell Stress Chaperones 17, 191–202.
Haque, A., Best, S.E., Ammerdorffer, A., Desbarrieres, L., de Oca, M.M., Amante, F.H., de Labastida Rivera, F., Hertzog, P., Boyle, G.M., Hill, G.R., et al., 2011. Type I interferons suppress CD4(+) T-cell-dependent parasite control during blood-stage Plasmodium infection. Eur. J. Immunol. 41, 2688–2698.
Hirunpetcharat, C., Finkelman, F., Clark, I.A., Good, M.F., 1999. Malaria parasite-specific Th1-like T cells simultaneously reduce parasitemia and promote disease. Parasite Immunol. 21, 319–329.
Holland, C.J., Cole, D.K., Godkin, A., 2013. Re-directing CD4(+) T cell responses with the flanking residues of MHC class II-bound peptides: the core is not enough. Front. Immunol. 4, 172.
Howick, V.M., Russell, A.J.C., Andrews, T., Heaton, H., Reid, A.J., Natarajan, K., Butungi, H., Metcalf, T., Verzier, L.H., Rayner, J.C., et al., 2019. The Malaria Cell Atlas: single parasite transcriptomes across the complete Plasmodium life cycle. Science 365.
Howland, S.W., Poh, C.M., Gun, S.Y., Claser, C., Malleret, B., Shastri, N., Ginhoux, F., Grotenbreg, G.M., Renia, L., 2013. Brain microvessel cross-presentation is a hallmark of experimental cerebral malaria. EMBO Mol. Med. 5, 984–999.
Hunt, D.F., Michel, H., Dickinson, T.A., Shabanowitz, J., Cox, A.L., Sakaguchi, K., Appella, E., Grey, H.M., Sette, A., 1992. Peptides presented to the immune system by the murine class II major histocompatibility complex molecule I-Ad. Science 256, 1817–1820.
James, K.R., Soon, M.S.F., Sebina, I., Fernandez-Ruiz, D., Davey, G., Liligeto, U.N., Nair, A.S., Fogg, L.G., Edwards, C.L., Best, S.E., et al., 2018. IFN regulatory factor 3 balances Th1 and T follicular helper immunity during nonlethal blood-stage Plasmodium infection. J. Immunol. 200, 1443–1456.
Kasahara, S., Clark, E.A., 2012. Dendritic cell-associated lectin 2 (DCAL2) defines a distinct CD8alpha- dendritic cell subset. J. Leukoc. Biol. 91, 437–448.
Kato, Y., Zaid, A., Davey, G.M., Mueller, S.N., Nutt, S.L., Zotos, D., Tarlinton, D.M., Shortman, K., Lahoud, M.H., Heath, W.R., et al., 2015. Targeting antigen to Clec9A primes follicular Th cell memory responses capable of robust recall. J. Immunol. 195, 1006–1014.
Kim, T.S., Jang, C.Y., Kim, H.D., Lee, J.Y., Ahn, B.Y., Kim, J., 2006. Interaction of Hsp90 with ribosomal proteins protects from ubiquitination and proteasome-dependent degradation. Mol. Biol. Cell 17, 824–833.
Krieg, A.M., 2006. Therapeutic potential of Toll-like receptor 9 activation. Nat. Rev. Drug Discov. 5, 471–484.
Lahoud, M.H., Ahmet, F., Kitsoulis, S., Wan, S.S., Vremec, D., Lee, C.N., Phipson, B., Shi, W., Smyth, G.K., Lew, A.M., et al., 2011. Targeting antigen to mouse dendritic cells via Clec9A induces potent CD4 T cell responses biased toward a follicular helper phenotype. J. Immunol. 187, 842–850.
Landais, E., Romagnoli, P.A., Corper, A.L., Shires, J., Altman, J.D., Wilson, I.A., Garcia, K.C., Teyton, L., 2009. New design of MHC class II tetramers to accommodate fundamental principles of antigen presentation. J. Immunol. 183, 7949–7957.
Langhorne, J., Gillard, S., Simon, B., Slade, S., Eichmann, K., 1989. Frequencies of CD4+ T cells reactive with Plasmodium chabaudi chabaudi: distinct response kinetics for cells with Th1 and Th2 characteristics during infection. Int. Immunol. 1, 416–424.
Langhorne, J., Simon-Haarhaus, B., Meding, S.J., 1990. The role of CD4+ T cells in the protective immune response to Plasmodium chabaudi in vivo. Immunol. Lett. 25, 101–107.
Langhorne, J., Cross, C., Seixas, E., Li, C., von der Weid, T., 1998. A role for B cells in the development of T cell helper function in a malaria infection in mice. Proc. Natl. Acad. Sci. U. S. A. 95, 1730–1734.
Li, C., Langhorne, J., 2000. Tumor necrosis factor alpha p55 receptor is important for development of memory responses to blood-stage malaria infection. Infect. Immun. 68, 5724–5730.
Lonnberg, T., Svensson, V., James, K.R., Fernandez-Ruiz, D., Sebina, I., Montandon, R., Soon, M.S., Fogg, L.G., Nair, A.S., Liligeto, U., et al., 2017. Single-cell RNA-seq and computational analysis using temporal mixture modelling resolves Th1/Tfh fate bifurcation in malaria. Sci. Immunol. 2.
Lundie, R.J., de Koning-Ward, T.F., Davey, G.M., Nie, C.Q., Hansen, D.S., Lau, L.S., Mintern, J.D., Belz, G.T., Schofield, L., Carbone, F.R., et al., 2008. Blood-stage Plasmodium infection induces CD8+ T lymphocytes to parasite-expressed antigens, largely regulated by CD8alpha+ dendritic cells. Proc. Natl. Acad. Sci. U. S. A. 105, 14509–14514.
Mach, N., Gillessen, S., Wilson, S.B., Sheehan, C., Mihm, M., Dranoff, G., 2000. Differences in dendritic cells stimulated in vivo by tumors engineered to secrete granulocyte-macrophage colony-stimulating factor or Flt3-ligand. Canc. Res. 60, 3239–3246.
McFarland, B.J., Sant, A.J., Lybrand, T.P., Beeson, C., 1999. Ovalbumin(323-339) peptide binds to the major histocompatibility complex class II I-A(d) protein using two functionally distinct registers. Biochemistry 38, 16663–16670.
Nelson, C.A., Petzold, S.J., Unanue, E.R., 1994. Peptides determine the lifespan of MHC class II molecules in the antigen-presenting cell. Nature 371, 250–252.
Nitcheu, J., Bonduelle, O., Combadiere, C., Tefit, M., Seilhean, D., Mazier, D., Combadiere, B., 2003. Perforin-dependent brain-infiltrating cytotoxic CD8+ T lymphocytes mediate experimental cerebral malaria pathogenesis. J. Immunol. 170, 2221–2228.
Oakley, M.S., Sahu, B.R., Lotspeich-Cole, L., Solanki, N.R., Majam, V., Pham, P.T., Banerjee, R., Kozakai, Y., Derrick, S.C., Kumar, S., et al., 2013. The transcription factor T-bet regulates parasitemia and promotes pathogenesis during Plasmodium berghei ANKA murine malaria. J. Immunol. 191, 4699–4708.
Oakley, M.S., Sahu, B.R., Lotspeich-Cole, L., Majam, V., Thao Pham, P., Sengupta Banerjee, A., Kozakai, Y., Morris, S.L., Kumar, S., 2014. T-bet modulates the antibody response and immune protection during murine malaria. Eur. J. Immunol. 44, 2680–2691.
Okabe, M., Ikawa, M., Kominami, K., Nakanishi, T., Nishimune, Y., 1997. 'Green mice' as a source of ubiquitous green cells. FEBS (Fed. Eur. Biochem. Soc.) Lett. 407, 313–319.
Pallavi, R., Roy, N., Nageshan, R.K., Talukdar, P., Pavithra, S.R., Reddy, R., Venketesh, S., Kumar, R., Gupta, A.K., Singh, R.K., et al., 2010. Heat shock protein 90 as a drug target against protozoan infections: biochemical characterization of HSP90 from Plasmodium falciparum and Trypanosoma evansi and evaluation of its inhibitor as a candidate drug. J. Biol. Chem. 285, 37964–37975.
Perez-Mazliah, D., Langhorne, J., 2014. CD4 T-cell subsets in malaria: TH1/TH2 revisited. Front. Immunol. 5, 671.
Perez-Mazliah, D., Ng, D.H., Freitas do Rosario, A.P., McLaughlin, S., Mastelic-Gavillet, B., Sodenkamp, J., Kushinga, G., Langhorne, J., 2015. Disruption of IL-21 signaling affects T cell-B cell interactions and abrogates protective humoral immunity to malaria. PLoS Pathog. 11, e1004715.
Perez-Mazliah, D., Nguyen, M.P., Hosking, C., McLaughlin, S., Lewis, M.D., Tumwine, I., Levy, P., Langhorne, J., 2017. Follicular helper T cells are essential for the elimination of Plasmodium infection. EBioMedicine 24, 216–230.
Pratt, W.B., 1997. The role of the hsp90-based chaperone system in signal transduction by nuclear receptors and receptors signaling via MAP kinase. Annu. Rev. Pharmacol. Toxicol. 37, 297–326.
Quin, S.J., Langhorne, J., 2001. Different regions of the malaria merozoite surface protein 1 of Plasmodium chabaudi elicit distinct T-cell and antibody isotype responses. Infect. Immun. 69, 2245–2251.
Salles, E.M., Menezes, M.N., Siqueira, R., Borges da Silva, H., Amaral, E.P., Castillo-Mendez, S.I., Cunha, I., Cassado, A.D.A., Vieira, F.S., Olivieri, D.N., et al., 2017. P2X7 receptor drives Th1 cell differentiation and controls the follicular helper T cell population to protect against Plasmodium chabaudi malaria. PLoS Pathog. 13, e1006595.
Samulowitz, U., Weber, M., Weeratna, R., Uhlmann, E., Noll, B., Krieg, A.M., Vollmer, J., 2010. A novel class of immune-stimulatory CpG oligodeoxynucleotides unifies high potency in type I interferon induction with preferred structural properties. Oligonucleotides 20, 93–101.
Sargeant, T.J., Marti, M., Caler, E., Carlton, J.M., Simpson, K., Speed, T.P., Cowman, A.F., 2006. Lineage-specific expansion of proteins exported to erythrocytes in malaria parasites. Genome Biol. 7, R12.
Schittenhelm, R.B., Sian, T.C., Wilmann, P.G., Dudek, N.L., Purcell, A.W., 2015. Revisiting the arthritogenic peptide theory: quantitative not qualitative changes in the peptide repertoire of HLA-B27 allotypes. Arthritis Rheum. 67, 702–713.
Schofield, L., Villaquiran, J., Ferreira, A., Schellekens, H., Nussenzweig, R., Nussenzweig, V., 1987. Gamma interferon, CD8+ T cells and antibodies required for immunity to malaria sporozoites. Nature 330, 664–666.
Smith, C.M., Belz, G.T., Wilson, N.S., Villadangos, J.A., Shortman, K., Carbone, F.R., Heath, W.R., 2003. Cutting edge: conventional CD8 alpha+ dendritic cells are preferentially involved in CTL priming after footpad infection with herpes simplex virus-1. J. Immunol. 170, 4437–4440.
Sponaas, A.M., Cadman, E.T., Voisine, C., Harrison, V., Boonstra, A., O'Garra, A., Langhorne, J., 2006. Malaria infection changes the ability of splenic dendritic cell populations to stimulate antigen-specific T cells. J. Exp. Med. 203, 1427–1433.
Stephens, R., Albano, F.R., Quin, S., Pascal, B.J., Harrison, V., Stockinger, B., Kioussis, D., Weltzien, H.U., Langhorne, J., 2005. Malaria-specific transgenic CD4(+) T cells protect immunodeficient mice from lethal infection and demonstrate requirement for a protective threshold of antibody production for parasite clearance. Blood 106, 1676–1684.
Su, Z., Stevenson, M.M., 2000. Central role of endogenous gamma interferon in protective immunity against blood-stage Plasmodium chabaudi AS infection. Infect. Immun. 68, 4399–4406.
Süss, G., Eichmann, K., Kury, E., Linke, A., Langhorne, J., 1988. Roles of CD4- and CD8-bearing T lymphocytes in the immune response to the erythrocytic stages of Plasmodium chabaudi. Infect. Immun. 56, 3081–3088.
Swanson 2nd, P.A., Hart, G.T., Russo, M.V., Nayak, D., Yazew, T., Pena, M., Khan, S.M., Janse, C.J., Pierce, S.K., McGavern, D.B., 2016. CD8+ T cells induce fatal brainstem pathology during cerebral malaria via luminal antigen-specific engagement of brain vasculature. PLoS Pathog. 12, e1006022.
Taylor-Robinson, A.W., Phillips, R.S., 1994. B cells are required for the switch from Th1- to Th2-regulated immune responses to Plasmodium chabaudi chabaudi infection. Infect. Immun. 62, 2490–2498.
Taylor-Robinson, A.W., Phillips, R.S., Severn, A., Moncada, S., Liew, F.Y., 1993. The role of TH1 and TH2 cells in a rodent malaria infection. Science 260, 1931–1934.

Teo, T.H., Howland, S.W., Claser, C., Gun, S.Y., Poh, C.M., Lee, W.W., Lum, F.M., Ng, L.F., Renia, L., 2018. Co-infection with Chikungunya virus alters trafficking of pathogenic CD8(+) T cells into the brain and prevents Plasmodium-induced neuropathology. EMBO Mol. Med. 10, 121–138.

Tsuji, M., Romero, P., Nussenzweig, R.S., Zavala, F., 1990. CD4+ cytolytic T cell clone confers protection against murine malaria. J. Exp. Med. 172, 1353–1357.

Valencia-Hernandez, A.M., Ng, W.Y., Ghazanfari, N., Ghilas, S., de Menezes, M.N., Holz, L.E., Huang, C., English, K., Naung, M., Tan, P.S., et al., 2020. A natural peptide antigen within the Plasmodium ribosomal protein RPL6 confers liver TRM cell-mediated immunity against malaria in mice. Cell Host Microbe 27, 950–962 e957.

van der Heyde, H.C., Pepper, B., Batchelder, J., Cigel, F., Weidanz, W.P., 1997. The time course of selected malarial infections in cytokine-deficient mice. Exp. Parasitol. 85, 206–213.

Villegas-Mendez, A., Greig, R., Shaw, T.N., de Souza, J.B., Gwyer Findlay, E., Stumhofer, J.S., Hafalla, J.C., Blount, D.G., Hunter, C.A., Riley, E.M., et al., 2012. IFN-gamma-producing CD4+ T cells promote experimental cerebral malaria by modulating CD8+ T cell accumulation within the brain. J. Immunol. 189, 968–979.

von der Weid, T., Kopf, M., Kohler, G., Langhorne, J., 1994. The immune response to Plasmodium chabaudi malaria in interleukin-4-deficient mice. Eur. J. Immunol. 24, 2285–2293.

Vremec, D., Pooley, J., Hochrein, H., Wu, L., Shortman, K., 2000. CD4 and CD8 expression by dendritic cell subtypes in mouse thymus and spleen. J. Immunol. 164, 2978–2986.

Weiss, W.R., Sedegah, M., Berzofsky, J.A., Hoffman, S.L., 1993. The role of CD4+ T cells in immunity to malaria sporozoites. J. Immunol. 151, 2690–2698.

Wikenheiser, D.J., Ghosh, D., Kennedy, B., Stumhofer, J.S., 2016. The costimulatory molecule ICOS regulates host Th1 and follicular Th cell differentiation in response to Plasmodium chabaudi chabaudi AS infection. J. Immunol. 196, 778–791.

Zander, R.A., Obeng-Adjei, N., Guthmiller, J.J., Kulu, D.I., Li, J., Ongoiba, A., Traore, B., Crompton, P.D., Butler, N.S., 2015. PD-1 Co-inhibitory and OX40 Co-stimulatory crosstalk regulates helper T cell differentiation and anti-plasmodium humoral immunity. Cell Host Microbe 17, 628–641.